

Design and Development of a Methanol Concentration Controller for Fuel Cells



Marius Viljoen

177139

A dissertation submitted in the fulfilment of the requirements for the
Magister Technologiae: Engineering: Electrical

Department:
Electronic Engineering
Faculty of Engineering and Technology
Vaal University of Technology
Vanderbijlpark

Supervisor: Prof HC vZ Pienaar

Date: December 2008

Declaration

I, Marius Viljoen declare that this project is my own, unaided work. It is being submitted for the requirements for the Magister Technologiae: Engineering: Electrical to the Department: Electronic Engineering at the Vaal University of Technology, Vanderbijlpark. It has not been submitted before for any assessment to any educational institution.

.....
Marius Viljoen

Date:.....

Acknowledgements

I hereby wish to express my gratitude to the following individuals who enabled this document to be completed successfully:

Prof HC vZ Pienaar for his guidance, motivation and patience while doing the research.

Telkom Centre of Excellence for funding the research.

Dedication

This dissertation is dedicated to the love of my life, Amanda, and my two children, Mariska and Francois, for their encouragement during the study of this project.

Abstract

The demand for higher efficiency, sustainability and cleaner power sources increases daily. A Direct Methanol Fuel Cell is a power source that can be applied for small to medium household appliances and office equipment. It can ideally be used for operating appliances like notebook computers on remote sites where no electrical power is available.

One of the problems in methanol fuel cells is methanol crossover. Methanol crossover occurs when methanol is not completely used in the process of generating electrons, and a certain percentage of the methanol is wasted. Crossover may damage the proton exchange membrane of the fuel cell and reduce the efficiency of a DMFC. Literature reviews were done and suggestions from other writers are discussed on how to reduce methanol crossover. This research focuses primarily on the fact that crossover can be controlled by controlling the methanol / water concentration.

A prototype methanol controller was built with an ultrasonic sensor for detecting the density of the methanol/water mixture and a sensor for the temperature of the mixture; this was done because the density of the mixture is dependant on the temperature and the concentration. The controller was calibrated to determine the amount per volume of water and methanol which enables the controller to control the percentage of methanol in the water. The prototype also had the feature built in to adjust the mixture in order to enable the study on the effects of crossover. A data logger function was added to store collected data on a personal computer for the study on methanol and water.

It was observed that the sensor was sensitive enough and was able to produce 1% increments of the level of methanol concentration in the water provided the temperature was stable. A methanol controller was successfully built to ensure the correct volume of methanol.

Table of contents

Declaration	ii
Acknowledgements	iii
Dedication	iv
Abstract	v
Table of contents	vi
List of Figures	viii
Glossary of Abbreviations and definitions	xi
CHAPTER 1 INTRODUCTION AND OVERVIEW	1
1.1 Background	1
1.2 Problem statement	4
1.3 Research methodology	4
1.4 Importance of the research	4
1.5 Overview of the research	5
1.6 Summary	5
CHAPTER 2 THEORETICAL CONSIDERATIONS	6
2.1 Introduction	6
2.2 Operation of a DMFC	7
2.3 Fuel crossover	11
2.4 Reducing fuel crossover	11
2.5 Concentration sensors	13
2.6 Temperature measurement	19
2.7 Flow control	19
2.8 Summary	21

CHAPTER 3	DESIGN OF A DMFC CONCENTRATION CONTROLLER	22
3.1	Introduction	22
3.2	Concentration controller assembly	22
3.3	The electronic design	26
3.4	Summary	28
CHAPTER 4	MEASUREMENTS AND RESULTS	29
4.1	Introduction	29
4.2	Temperature calibration	29
4.3	The detector voltage calibration	31
4.4	Temperature effects on the detector	32
4.5	Testing stability of the detector	35
4.6	Comparing different concentration mixes at the same temperature.	37
4.7	Comparing concentration mixes of the detector	39
4.8	Summary	41
CHAPTER 5	CONCLUSION AND RECOMMENDATIONS	42
5.1	Concluding comments	42
5.2	Conclusions attained from the study	42
5.3	Recommendations	45
5.4	Other applications	45
REFERENCES		46
ANNEXURE A	PIC SOURCE CODE FOR THE CONTROLLER	49
ANNEXURE B	MURATA SENSOR DATA SHEET	55

List of Figures

Figure 1: A 50-Watt DMFC system manufactured by Smart Fuel Cell Inc.	3
Figure 2: Laptop with a local power supply from a fuel cell (Toshiba)	4
Figure 3: Parts of a fuel cell (Nice)	8
Figure 4: Flow of chemicals in the DMFC (Nice)	9
Figure 5: Schematic of a DMFC	10
Figure 6: Graph showing how the crossover of methanol to the cathode changes with fuel concentration. (Ren, Zelanay et al.)	13
Figure 7: A typical pH sensor (Griffiths)	14
Figure 8: A typical setup for a four electrode conductivity meter (Mettler-Toledo Thornton Inc.)	15
Figure 9: Methanol sensor based on electrochemical oxidation of methanol coupled with electrochemical reduction of water (Nasa's Tech Briefs)	16
Figure 10: Sensata Methonal Concentration Sensor (MCS) (Texas Instruments)	17
Figure 11: Refractive index of aqueous methanol solutions of a Sensata sensor	18
Figure 12: Murata's ultrasonic sensor	18
Figure 13: Typical configuration for the DS18X20 temperature sensors	19
Figure 14: Pulse width modulation setup	21
Figure 15: Experimental set-up for optical sensing system (Sung Min Cho et al.)	23
Figure 16: Acoustic configuration of the sensor (Murata Manufacturing Co. Ltd)	24
Figure 17: General view of the sensor (Murata Manufacturing Co. Ltd)	25
Figure 18: Driving signal voltage and received sound pressure (Murata Manufacturing Co Ltd)	25
Figure 19: Flow diagram of the methanol controller software	26
Figure 20: Basic layout of the methanol concentration tester	27
Figure 21: Layout of the prototype	28
Figure 22: Basic layout of the sensor liquid circuit	29
Figure 23: Measurement of temperature against A/D values obtained from the detector	30
Figure 24: Voltage values measured on ultrasonic detector versus A/D values read by the microprocessor	32
Figure 25: Density versus temperature of pure water	33
Figure 26: Detector values versus temperature of pure water	34
Figure 27: Detector values versus temperature of pure water on a slow cool down test	35
Figure 28: 4% by volume methanol mix on a slow cool down test repeated 3 times	36
Figure 29: Varying circulation speed readings to test stability	37
Figure 30: Testing concentration mix at a constant temperature	37
Figure 31: Varying circulation speed readings to test stability	38
Figure 32: LCD display of the prototype	40

Figure 33: Comparison of different water methanol mix samples changing temperature over time	41
Figure 34: Measurement data of V_{DET} value by temperature and concentration of methanol (Murata Co. Ltd)	43
Figure 35: Sound velocity of methanol	44
Figure 36: Sound velocity of methanol vs concentration	44

List of tables

Table 1: Calibration Values for temperature	30
Table 2: Voltage values measured on detector versus A/D values read by the microprocessor	31
Table 3: Density table of water (www.Simetrix.co.uk)	33
Table 4: Temperature comparison table	39

Glossary of Abbreviations and definitions

A

AFC: alkaline fuel cell

ADC: analogue to digital converter

C

Composite: Synthetic material made of various constituents

Convection: Circulatory motion that occurs in a fluid at a non-uniform temperature

Crossover: Wasted fuel that migrates through the electrolyte

D

DC: Direct Current

DMFC: direct methanol fuel cell

E

e^- : electron

F

FC: Fuel cell

Flooding: Excess water covering active areas of the cell

H

Heterogeneous: Diverse in character or made of different kinds of materials

M

MEA: Membrane electrode assembly

Mole: The amount of a substance that contains as many atoms, molecules, ions, or other elementary units as the number of atoms in 0.012 kilogram of carbon 12. The number is 6.0225×10^{23} , or Avogadro's number

N

Nafion®: Proton exchange membrane developed by the Dupont™ company

P

PCB: Printed circuit board

PEM: Proton exchange membrane

PEMFC: Proton exchange membrane fuel Cell

Pt: Platinum

PTFE: Teflon

Purging: Removal of 'old' reactants from the active area by an influx of a reactant or a sudden pressure drop

PVDF: Polyvinylidene fluoride

PWM: Pulse width modulation

R

Regenerative: The ability of a device to produce the fuel it will later consume

Ru: Ruthenium

U

Utilisation: Effective use of the reactant

Chapter 1 Introduction and Overview

1.1 Background

The global demand for energy is rising constantly. However, fossil energy resources - such as oil, coal and gas - are not inexhaustible. While the world economy continues to grow under these preconditions, increasingly scarce oil reserves will continue to push up energy prices. Despite the many optimistic forecasts, the price of a barrel of oil rose to over 140 dollars in 2008. Whether we like it or not, the current situation compels us to seek new solutions. Given the present state of technology, the energy crises can only be avoided by saving energy and generating it more efficiently. This, in turn, will also help to curb the greenhouse effect (Fuel Cell Info-CD II 2008).

Energy has always been one of the main concerns of humankind. Its importance and the need for energy have been increasing with increasing world population and growing industry. In the 1900s, with the Industrial Revolution, energy shortage became a big problem. To address this problem the number of power plants increased dramatically to produce more energy, and this led to new problems. Coal power plants, nuclear plants, combustion engines and hydroelectric power plants caused problems such as air pollution, noise pollution, lack of efficiency, high cost and fatal danger. Researchers started to think about new power supply systems with less noise, emissions and danger yet with a high efficiency (Ayhan 2002:1).

According to many news reports, new energy-saving technology to generate electrical power for our homes and cars may be used in the near future. Technology development in this regard is of extreme importance to the human population because it offers a means of making power available more efficiently and with less pollution.

Fuel cells seem to be a solution for the supply of clean, efficient and non-hazardous energy. Luigi Galvani (1737-1798) was the first to formulate the assumption that chemical energy can be directly converted into electrical energy and that this process is reversible. His theory of electrochemical conversion provides the basis for the subsequent development of fuel-cells and electrolyzers (Geitman 2004:34).

According to Larminie and Dicks (2003:1) the first demonstration of a fuel cell was by a lawyer and scientist, William Grove, in 1839. After that a significant time elapsed before any new technological development was fully exploited. Ludwig Mond and Carl Langer produced the first fuel cell in 1889. In the next century, there were great efforts to improve fuel cell systems. Although the fuel cell has taken longer to develop than most other power systems and despite the promise of clean and efficient power generation we nowadays have high efficiency fuel cells are

available for many applications. These energy conversion devices still have problems and they need to be improved (Ayhan 2002:1)

According to Dr G Acres, Research Director at Johnson Matthey PLC, fuel cells were successfully developed for the American manned space programme in the 1950s. This success, together with a policy to commercialise space technology, led to substantial development programmes in America and Japan in the 1970s and the 1980s and more recently in Europe. During the last few years much has changed to stimulate new and expanding interest in fuel cell technology. Environmental concerns about global warming and the need to reduce CO₂ emissions provided the stimulus to seek ways of improving energy conversion efficiencies. The motor vehicle industry, apart from seeking higher fuel efficiencies, is also required to pursue technologies capable of eliminating emissions, the ultimate goal being the zero emission from cars.

A fuel cell is an **electrochemical energy conversion device** much like a battery except that is easily refuelled because the fuel is stored outside the cells. With a fuel cell, fuel constantly flows through the cell and is easily replenished outside the cell, so it never stops providing electrical current. As long as there is a flow of fuel through the cell, the electricity flows out of the cell. A fuel cell is an energy-**producing** device while a battery is an energy-**storing** device. With batteries the fuel is stored inside the battery and cannot easily be replenished. Most fuel cells in use today use hydrogen and oxygen as the chemical fuel. A fuel cell provides a DC voltage that can be used to power motors, lights or other DC electrical appliances. The DC voltage can also be inverted to a more usable AC voltage (Nice).

Conventional power generation systems transform chemical energy of a fuel into useful electrical or mechanical power with an intermediate step of heat production. Heat is mainly generated by combustion, nuclear or other reaction processes, which are responsible for significant energy loss. Fuel cells are a remarkable alternative for power generation transforming chemical energy directly into electric power and achieving higher efficiencies than conventional power generation systems. According to Hotz et al. a promising application of fuel cells are fuel cell micropower plants generating electric power in the order of a few watts to power mobile devices such as cell phones, cameras and notebooks. Fuel cell micropower plants have the potential to replace rechargeable batteries used in mobile devices today.

The highest performance of polymer electrolyte fuel cells (PEFC) can be achieved by using pure hydrogen as a fuel. However, the storage of hydrogen causes problems that have not yet been completely solved. Especially for fuel cell micropower plants, a common solution is the on-board production of hydrogen by reforming or processing a hydrocarbon fuel.

The preferred fuel for a fuel cell is hydrogen since it is an environment friendly fuel or gas but the problem is that hydrogen has the lowest viscosity and density of all gasses. This means that hydrogen has a high leak rate and will leak through very small orifices faster than any other gas. According to Larminie and Dicks (2003:280) hydrogen is also a highly volatile and flammable gas and in certain circumstances hydrogen and air mixtures can detonate.

Methanol is a low cost chemical and a readily available liquid fuel that has an energy density not very different from petroleum. According to Larminie and Dicks (2003:141) the Direct Methanol Fuel Cell (DMFC) is a simple system and easy to refill and this is one of the most important advantages!



Figure 1: A 50-Watt DMFC system manufactured by Smart Fuel Cell Inc.

Portable applications for DMFCs include emergency power supplies and local power supplies for devices such as laptops and camcorders, mobile telephones and construction site traffic lights. In principle, fuel cells can be used instead of standard batteries. However, if they are to replace them the fuel cells must be small, powerful and competitive. The first such products are already available on the market (Geitmann 2004:34).



Figure 2: Laptop with a local power supply from a fuel cell (Toshiba)

1.2 Problem statement

The purpose of this research is to design a micro-processor variable control system to measure and control the methanol concentration in a direct methanol fuel cell in order to reduce methanol crossover. This is done to extend the lifetime and improve the output of the fuel cell.

1.3 Research methodology

The research involves the theoretical study of the development and design of a variable control system for a DMFC in order to reduce fuel crossover.

A practical design and prototype product of a micro-controlled system is necessary to accomplish the design specifications as set out in the objectives.

Testing, measurements and calibration in a laboratory assist to ensure the working of the concentration control unit.

1.4 Importance of the research

The main objective of this research was to design a cost-effective micro-processor control system by using methanol density sensors and temperature sensors to monitor and control the methanol concentration in a DMFC system in order to reduce the fuel crossover in a cell and ultimately to ensure less maintenance on the cell because of extended life expectancy of the membrane.

The concentration control system should also ensure that DMFCs can be maintained without personal attention. The design of this device will be applied in the further study into the development of a portable DMFC.

1.5 Overview of the research

The design of the Methanol Concentration Controller is divided into four defined stages of thought.

The first stage, Chapter 2, involves the initial literature review and careful comprehension of the working of a DMFC. This study also includes a literature review on different types of concentration sensors and liquid temperature measurement.

Chapter 3 focuses on the physical design of the concentration controller and the working of the ultrasonic concentration sensor.

Chapter 4 involves the measurements and tests conducted in order to calibrate the concentration sensor. The results are then analysed to derive the design algorithms.

Chapter 5 contains the conclusions and recommendations obtained from the study and design of the concentration controller.

1.6 Summary

In this chapter the background to the need to control the methanol concentration in a DMFC and application thereof was provided. The purpose of the study along with the topic of research has been given. In conclusion, an overview of the research was presented.

In Chapter 2 the physical working of a DMFC will be investigated and an in-depth look at different commercial sensors will also be given.

Chapter 2 Theoretical Considerations

2.1 Introduction

To have a better understanding of the operation of a DMFC the main types of fuel cells available are briefly discussed. There are several different types of fuel cells, each using a different chemistry. Fuel cells are usually classified by the type of **electrolyte** they use. Some types of fuel cells work well for use in stationary power generation plants, others may be useful for small portable applications or for powering cars.

According to Nice (<http://science.howstuffworks.com/fuel-cell.htm>) fuel cells are classified into six categories:

- **Proton exchange membrane fuel cell (PEMFC):** This is a fuel cell which converts the chemicals, pure hydrogen and oxygen, into water, and in the process it produces electricity and heat. The application is for vehicles and mobile application and operates at about 30-100°C (Larminie & Dicks 2005:15).
- **Alkaline fuel cell (AFC):** This is one of the oldest designs. It has been used in the NASA Space program since the 1960s. The AFC is very susceptible to contamination, so it requires pure hydrogen and oxygen (hydrogen 99.9% pure). It is also very expensive, so this type of fuel cell is unlikely to be commercialised.
- **Phosphoric-acid fuel cell (PAFC):** The phosphoric-acid fuel cell has potential for use in small stationary power-generation systems. It operates at a higher temperature (150° - 200° C) than PEM fuel cells, so it has a longer warm-up time. This makes it unsuitable for use in cars.
- **Solid oxide fuel cell (SOFC):** These fuel cells are best suited for large-scale stationary power generators that could provide electricity for factories or towns. This type of fuel cell operates at very high temperatures around 1000°C. This high temperature makes reliability a problem, but it also has an advantage:—The steam produced by the fuel cell can be channelled to turbines to generate more electricity in the conventional manner. This improves the overall efficiency of the system.
- **Molten carbonate fuel cell (MCFC):** These fuel cells are also best suited for large stationary power generators. They operate at 600°C, so they also generate steam that can be used to generate more power. They have a lower operating temperature than the SOFC, which means that non-precious metals can be used instead of precious metals. This makes the design a little less expensive.
- **Direct methanol fuel cell (DMFC):** These fuel cells are best suited for portable electronic systems of low power, running for long times. The DMFC is also a PEM fuel

cell except that it uses a slightly thicker membrane and the membrane is not only treated with platinum but also with ruthenium. The operating temperature is between 20-90°C according to Larminie and Dicks (2005:15).

This study will focus on the last named fuel cell namely the DMFC. According to Larminie and Dicks(2005:141) the net energy density of methanol is higher than any of the other storage technologies used in hydrogen systems and another advantage is that it is faster to refill and easy to use.

Fuel cells are used as stacks for practical applications since the output of a single cell does not produce a high enough voltage. One notable problem associated with fuel cell stacks is the poor distribution of the reactants, which causes a decrease in efficiency and sometimes damage to the system itself. The biggest problem however with the DMFC is that the methanol anode reactions proceed slower than with hydrogen which results in the fact that the DMFC will give out less power for a given size. Another major problem is that of fuel crossover and this will be the focus of this research.

Although the electrolyte of a fuel cell would have been chosen for its ion conducting properties, it will always be able to support very small amounts of electron conduction. The situation is akin to minority carrier conduction in semiconductors. Some fuels will diffuse from the anode through the electrolyte to the cathode. Because of the catalyst, it will react directly with the oxygen, producing no current from the cell. This small amount of wasted fuel is known as fuel crossover (Larminie and Dicks 2005:53).

Larminie and Dicks (2005:142) also mention that the result of both these problems is that the performance of a DMFC is markedly worse than other types of fuel cells; if these problems could be addressed then the DMFC could also be used in mobile fuel cell applications.

2.2 Operation of a DMFC

The direct methanol fuel cell is based on the direct electro-oxidation of an aqueous solution of methanol in a polymer electrolyte membrane fuel cell without the use of a fuel processor. With the direct methanol fuel cell system, the complexity of processing the methanol into hydrogen is eliminated. A DMFC works by creating thermodynamic potential out of the chemical reaction between methanol and air without the aid of moving parts. DMFCs produce electricity through an electrochemical process, without combustion and without the need to reform the fuel stock into hydrogen or expose hydrogen in a gaseous state to the proton exchange membrane (PEM). The advantage of a DMFC over a traditional battery is that a DMFC can simply be refilled with more fuel when it runs out. DMFCs only require externally added fuel to run. As long as fuel and air are

supplied to the DMFC, it will continue to produce power. It does not need to be recharged (DTI ENERGY INC.).

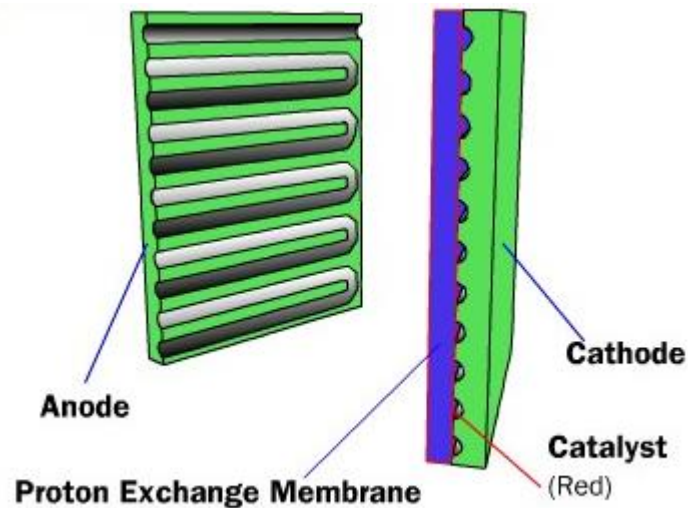


Figure 3: Parts of a fuel cell (Nice)

The **proton exchange membrane fuel cell** (PEMFC) uses one of the simplest reactions of any fuel cell.

Figure 3 shows the four basic elements of a PEMFC:

- The **anode**, the negative electrode of the fuel cell, has several functions. It conducts the electrons that are freed from the hydrogen molecules so that they can be used in an external circuit. It has channels etched into it that disperse the hydrogen gas equally over the surface of the catalyst.
- The **cathode**, the positive electrode of the fuel cell, has channels etched into it that distribute the oxygen to the surface of the catalyst. It also conducts the electrons back from the external circuit to the catalyst, where they can recombine with the hydrogen ions and oxygen to form water.
- The **electrolyte** is the PEM. This specially treated material, which looks something like ordinary kitchen plastic wrap, only conducts positively charged ions. The membrane blocks electrons.
- The **catalyst** is a special material which is usually made of platinum powder very thinly coated onto carbon paper. The platinum helps to obtain higher catalytic activity in the reaction of oxygen and hydrogen. It also helps to reduce the poisoning of the electrolyte by impure gases. The catalyst is rough and porous so that the maximum surface area of the platinum can be exposed to the hydrogen or oxygen. The platinum-coated side of the

membrane faces the PEM. The electro oxidation of methanol occurs on the platinum-ruthenium catalyst at the anode and the electro-reduction of oxygen occurs on the platinum catalyst at the cathode. **Ruthenium** is known as the most active oxide for anodic oxygen evolution.

Methanol fuel cells have demonstrated fuel-to-electric efficiencies in the range of 25-30% and this is about 50% of what can be realized with hydrogen-air fuel cells. However, in spite of the lower efficiencies of the direct methanol fuel cell, this fuel cell system with its compact fuel storage can compete in mass and volume with state-of-art hydrogen-air systems (Narayanan 2006:2).

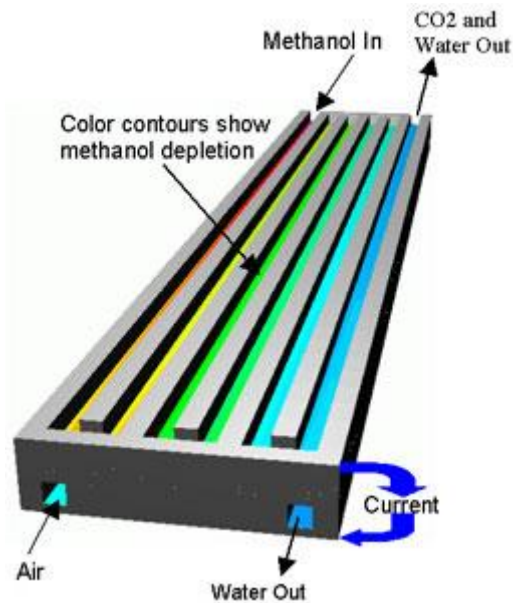


Figure 4: Flow of chemicals in the DMFC (Nice)

Direct Methanol Fuel Cells (DMFCs) utilize a membrane as an electrolyte and produce electricity directly from liquid methanol, eliminating the need for a fuel reformer. Figures 4 and 5 show the path of the methanol and that of the oxygen inside the cell. It can be seen that when the methanol reaches the catalyst, electrons are produced and the positive hydrogen atoms are going through the PEM.

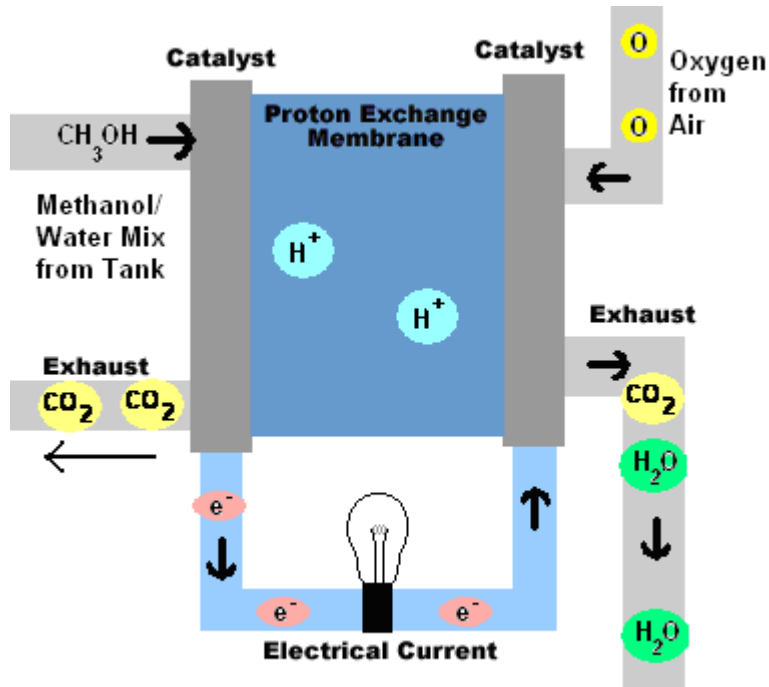
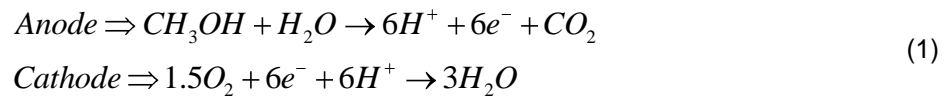


Figure 5: Schematic of a DMFC

The electrons produced in the reaction at the anode are first passed through the electronic load before reaching the cathode. In DMFCs, which use a methanol/water solution as fuel, the reactions can be described as follows:



The anode reaction produces an electrical current and protons migrate through the membrane electrode assembly (MEA). However, unlike the case of directly using hydrogen as a fuel, carbon dioxide is produced on the anode and is expelled along with excess water (Leahy 2004:10).

According to Larminie and Dicks (2005:30) six electrons are transferred for each molecule of methanol and the output voltage of a cell is 1.21V. The fuel cell will operate at efficiencies of above 40% at temperatures of 50–100°C. The efficiency will improve at higher temperatures.

According to Larminie and Dicks (2005:149) the loss of methanol is often transposed into “cross-over current” – the current equivalent to that, which would be produced by the methanol, had it reacted properly on the fuel anode.

DMFCs have a number of disadvantages i.e.:

- a) Firstly the fuel-anode reactions proceed slower than in the case of pure hydrogen. The oxidation of hydrogen occurs readily – the oxidation of methanol is a much more complex reaction and this results in a fuel cell with far lower power density for a given size.
- b) The second is that of methanol crossover. There is always a small amount of wasted fuel that migrates through the electrolyte to the cathode and this is called fuel crossover.

2.3 Fuel crossover

Methanol crossover is one of the primary performance limitations of direct methanol cells and it is more severe in direct methanol fuel cells. Methanol crossover occurs when methanol from the anode of the cell migrates through the electrolyte (methanol-permeable membrane) to the cathode. At the cathode, the methanol is able to react chemically with air. That is, the methanol can burn. This not only reduces the amount of oxygen to the cathode to drive electro-oxidation of methanol, but the combustion of methanol can have a harmful effect on the membrane and the rest of the cell's structure (Leahy 2004:39).

Internal currents and fuel crossover are essentially equivalent (Larmine & Dicks 2005:54). The current density will be small, typically only a few mA cm^{-2} . With low temperature cells this causes a very noticeable voltage drop at open circuit.

In the DMFC with a PEM electrolyte fuel crossover is severe, the reason is that methanol mixes very readily with water, and so spreads into the water that is an essential part of the structure of the PEM electrolyte. The methanol will thus reach the air cathode. This has a platinum catalyst, and although it will not oxidize the fuel as effectively as the Pt/Ru catalyst on the anode, it will do so fairly readily. The reaction of the fuel at the cathode is not only a waste of fuel – it will also reduce the cell voltage.

2.4 Reducing fuel crossover

Among the critical problems remaining to be solved in the improvement of the DMFC performance are the slow anode kinetics, methanol crossover through the polymer electrolyte, gas management at the anode, and water management on the cathode. The deleterious methanol crossover from anode to cathode significantly reduces the open circuit voltage as well as fuel efficiency. Narayanan et al.(2006) reported on the influence of the Nafion® membrane thickness on methanol crossover rate. Narayanan et al.(2006:2) found methanol crossover was affected by temperature and indicated the crossover effect increased with cell temperature.

The MEAs are constructed from a proton exchange membrane such as Nafion 117 (Du Pont) with a thickness of 0.01778 mm on to which catalyst layers consisting of noble metal catalysts are applied. Platinum-ruthenium (Johnson-Matthey High Spec 6000) is a widely-used catalyst for the oxidation of methanol, and platinum-black (Johnson-Matthey, fuel cell grade) is a commonly-used catalyst for the cathode. Catalyst loading levels as high as 8 mg/cm² are used on each electrode to achieve high performance. For a viable system design that maintains thermal and water balance, the performance of the cell at 60°C at low flow rates of air is very important. Performance at low air flow rates is limited by the demands for air from methanol crossing over to the cathode, the carbon dioxide blanket created by the crossover reaction and the large quantities of liquid water that are drawn across the cell by the electro-osmotic transport process. To overcome these limitations, MEAs are usually operated at three to four times the stoichiometric flow rates. This limits the system design from not being able to operate in environments that are hotter than 40°C (Narayanan et al. 2006:2-4).

Heinzel and Barragan (1999:70-74) gave an extensive review of methanol crossover in direct methanol fuel cells, enumerating various parameters influencing methanol crossover, such as methanol concentration, pressure, temperature, membrane thickness, and catalyst morphology. Ren, Springer et al (2000:86) used lower methanol concentrations and optimized cell design to decrease methanol crossover in their fuel cell systems. Gurau and Smotkin (2002:344) extensively characterized methanol crossover by gas chromatography.

Larmine and Dicks (2005:149) state that there are four principle methods that DMFC designers use to reduce fuel crossover:

- The anode catalyst is made as active as possible, within the bounds of reasonable cost. This results in the methanol reacting properly at the anode and not being available to diffuse through the electrolyte and on to the cathode.
- The fuel feed to the anode is controlled, so that at times of low current there is no excess of methanol. The concentration should always be about 1 mole depending on the fuel cell.
- Thicker electrolytes than normal for PEMFCs are used. This will reduce fuel crossover but will increase the cell resistance.
- The composition of the PEM also has an effect. It has been shown by Ren, Springer and Gottesfeld (2000:92-98) that the diffusion and water uptake for 1100 EW Nafion is about half of that for 1200 EW Nafion.

This research focuses on point two mentioned above, namely to control the concentration and the flow rate of the methanol/water mixture.

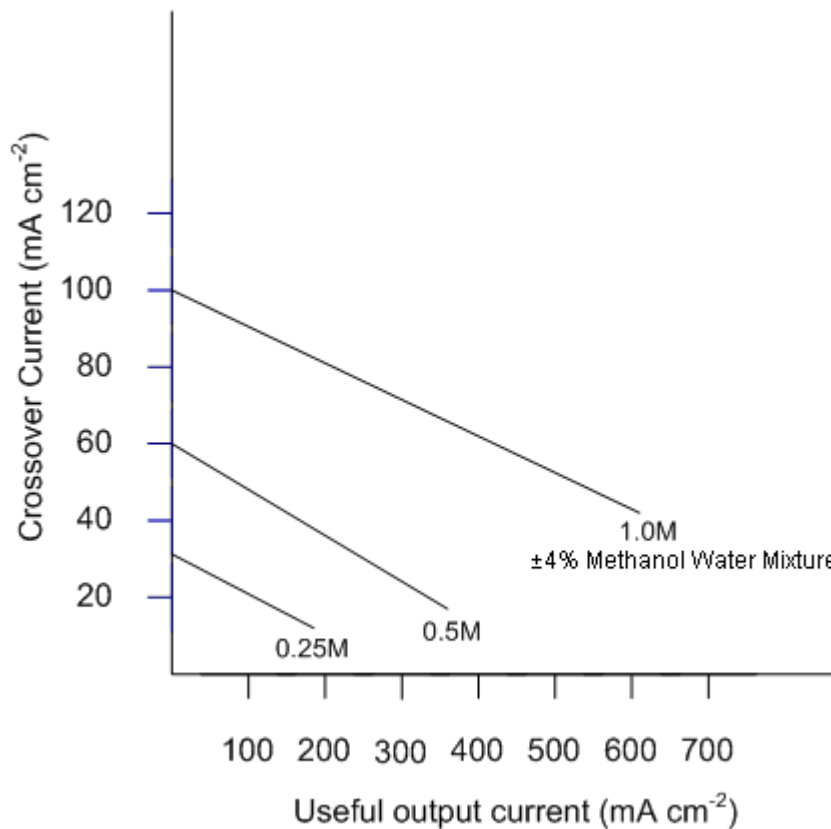


Figure 6: Graph showing how the crossover of methanol to the cathode changes with fuel concentration. (Ren, Zelanay et al.)

Figure 6 shows the crossover current of methanol from anode to cathode through the membrane with respect to the useful output current. Fuel crossover reduces as the current from the cell increases as can be seen from the graph above. It is therefore helpful if the methanol fuel cell is designed to run at more or less maximum power. To do this, it will be necessary to use a super capacitor or a small rechargeable battery to ensure a constant load. Another option would be to control the concentration of the methanol in the water to adjust for higher or lower currents.

2.5 Concentration sensors

Measurement of methanol concentration in real time during DMFC system operation is important for maintaining constant methanol concentration and ensuring uniform system performance. The concentration of methanol is dropped by continuous power generation in the system. Therefore, the system must be capable of detecting the concentration in situ, to calculate the amount of fresh methanol to be added, and to supply fresh methanol to the anode sides.

2.5.1 pH sensing

The pH of a solution indicates how acidic or basic (alkaline) it is. The pH term translates the values of the hydrogen ion concentration - which ordinarily ranges between about 1 and 10^{-14} gram-equivalents per litre - into numbers between 0 and 14.

On the pH scale a very acidic solution has a low pH value such as 0, 1, or 2 (which corresponds to a large concentration of hydrogen ions— 10^0 , 10^{-1} , or 10^{-2} gram-equivalents per litre) while a very basic solution has a high pH value, such as 12, 13, or 14 which corresponds to a small number of hydrogen ions (10^{-12} , 10^{-13} , or 10^{-14} gram-equivalents per litre). A neutral solution such as water has a pH of approximately 7 (Griffiths).

A pH measurement loop is made up of three components— the first is the pH sensor, which includes a measuring electrode, a reference electrode, and a temperature sensor, the second a preamplifier, and the third an analyser or transmitter. A pH measurement loop is essentially a battery where the positive terminal is the measuring electrode and the negative terminal is the reference electrode. The measuring electrode, which is sensitive to the hydrogen ion, develops a potential (voltage) directly related to the hydrogen ion concentration of the solution. The reference electrode provides a stable potential against which the measuring electrode can be compared.

The reason for discussing this type of sensor is that it can also be an indication for the density of the solution as can be seen when looking at the equation definition for pH which is as follows:

$$pH \approx -\log_{10} \frac{[H^+]}{1 \text{ mol} / L} \quad (2)$$

In dilute solutions such as tap water, activity is approximately equal to the numeric value of the concentration of the H^+ ion.



Figure 7: A typical pH sensor (Griffiths)

2.5.2 Conductivity measurement

Electrical conductivity is the ability of a material to carry electrical current. In water, it is generally used as a measure of the mineral or other ionic concentration. Conductivity is a measure of the purity of water or the **concentration** of ionized chemicals in water. However, conductivity is only a quantitative measurement– it responds to all ionic content and cannot distinguish particular conductive materials in the presence of others.

Only ionisable materials will contribute to conductivity; materials such as sugars or oils are not conductive. In a metal conductor, electrical current is the flow of electrons and is called *electronic* conductance. In water, electrical current is carried by ions since electrons do not pass through water by themselves. This is *electrolytic* conductance (Mettler-Toledo Thornton Inc.)

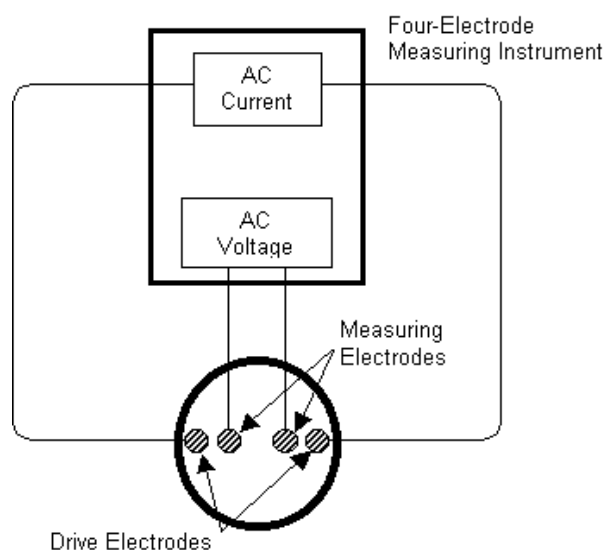


Figure 8: A typical setup for a four electrode conductivity meter (Mettler-Toledo Thornton Inc.)

There are various conductivity sensors some of which make use of a toroidal transformer.

2.5.3 Sensors based on electrochemical oxidation.

Nasa has developed a sensor based on the electrochemical oxidation of methanol. The sensor is expected to be particularly useful in continuous monitoring and control of the concentration of an aqueous solution of methanol metered into a liquid-feed, direct-oxidation methanol fuel cell.

It is stated that it also offers a wide dynamic range; it can measure concentrations from 0.01 M to 5 M. Furthermore, it functions over the entire temperature range of liquid water at normal atmospheric pressure, that is, from 0 to 100 °C.

The sensor (see Figure 9) resembles a small liquid-feed, direct-oxidation fuel cell in some respects, but is operated as a regeneration fuel cell. It includes a polymer-electrolyte membrane coated on one side with a catalytic electrode composed of Pt/Ru-alloy powder and coated on the other side with a catalytic electrode composed of Pt black. Some details of the preparation of the Pt/Ru powder, the polymer-electrolyte membrane, and coating the membrane with the Pt/Ru powder were described in NASA's Tech Briefs, Vol. 20, No. 10, 1996:60. The coated membrane is pressed between sheets of the porous carbon paper. The resulting sandwich is mounted between graphite plates that act as both current collectors and structural supports. Circular openings in the graphite plates expose the sandwich to the aqueous solution of methanol.

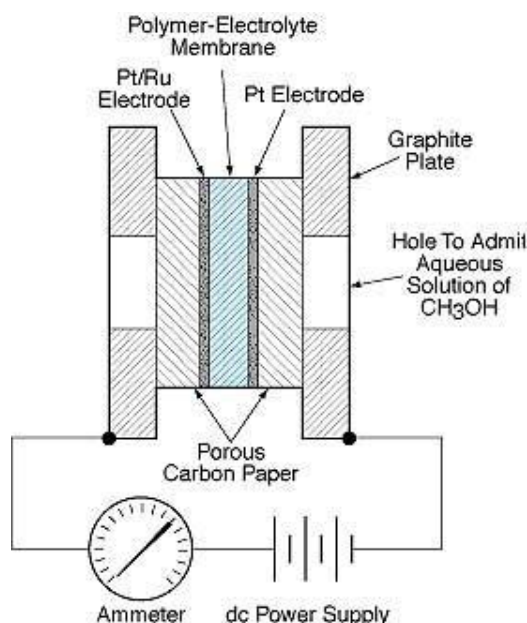


Figure 9: Methanol sensor based on electrochemical oxidation of methanol coupled with electrochemical reduction of water (Nasa's Tech Briefs)

As the applied potential increases, the rate of this reaction (and thus the electric current) becomes subject to limitation on the rate of transport of methanol to the surface of the Pt/Ru electrode. As the concentration of methanol increases, more methanol becomes available for transport, making it possible to sustain a larger transport-limited current. Thus, for a given applied potential, the current increases with the concentration of methanol. This behaviour is exploited in designing the methanol sensor; in the basic mode of operation, one applies a specified potential in the range in which current is strongly transport-limited (e.g. 0.63 V) and measures the current as an indication of the concentration of methanol.

The response of the sensor also depends on temperature. At each operating temperature of interest, the sensor is calibrated by applying the potential and measuring the current in the presence of aqueous solutions with known concentrations of methanol (Nasa Tech Briefs).

2.5.4 Optical sensors

Optical fuel composition sensors measure the refractive index of the fuel using one of two methods. The first method uses detection of the changes in the amount of light that is received by a receiving element and the second method uses measurement of the change in the direction of an incident light beam onto a receiving element based on Snell's law (Suzuki and Ogawa 1991:1).

The first method has not found wide acceptance because it is generally too sensitive to contamination of the optical system. Sung Min Cho et al. (2007:1) developed a methanol sensing system composed of a collimated laser beam, a triangle shaped quartz, two photo detectors and a control circuit in order to measure the refraction angles for various methanol concentrations (Figure 15 on p.23 in Chapter 3). The laser beam passes the quartz filled with the current concentration and hits two detectors, then the control circuit collects the voltages from the refraction angles, converts them to the digital values through the ADC. This sensing system resolves extremely small changes in concentration, in the order of 0.01%, while providing a large dynamic measurement range (0~100% methanol concentration). After the methanol sensor is connected to the stack, it can detect in real time the current methanol concentration and supply the accurate amount of fresh methanol without human intervention.

Sensata Technologies Methanol Concentration Sensor (Figure 10) is another optical sensing device for real time methanol concentration analysis and is distributed by Texas Instruments. This sensor is a miniaturized, self-contained optical system that measures the refractive index of aqueous methanol samples rapidly and affordably. The patented sensor design enables in-line process control for methanol-based fuel systems.



Figure 10: Sensata Methanol Concentration Sensor (MCS) (Texas Instruments)

The main advantage of this system is that the values obtained of the refractive index curve are linear with the change in methanol concentration as can be seen in Figure 11.

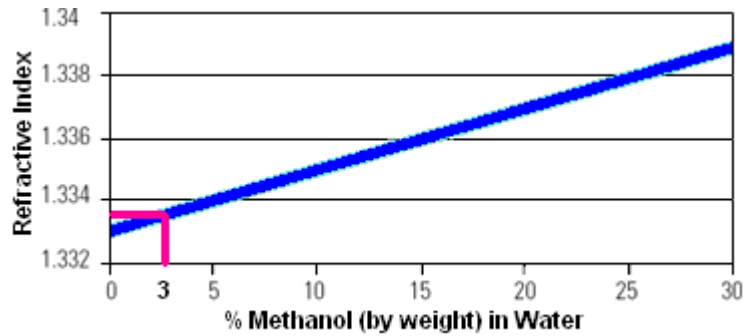


Figure 11: Refractive index of aqueous methanol solutions of a Sensata sensor

2.5.5 Ultrasonic sensors

The velocity of sound in a solution changes with a change in concentration and temperature of the methanol mixture. The concentration can be detected by measuring the velocity of sound as well as the temperature of the solution. Murata Manufacturing Co Ltd has commercialized a small, high-precision methanol concentration sensor. This sensor can be applied to measure methanol levels in DMFCs.

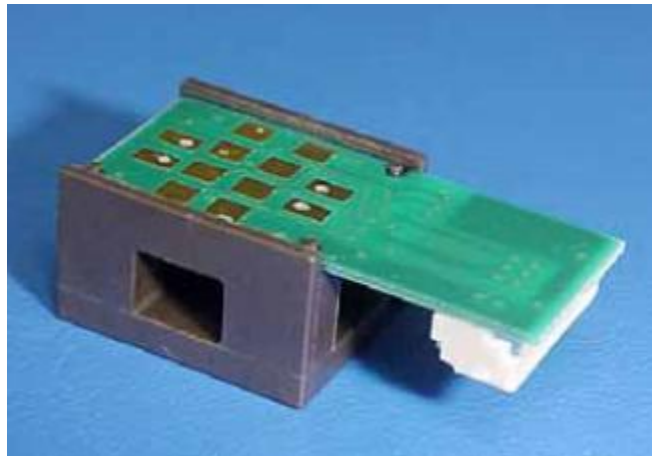


Figure 12: Murata's ultrasonic sensor

The sound velocity at which ultrasonic waves propagate through methanol solutions depends on the methanol mix concentration and the temperature. Murata have developed a methanol concentration sensor that measures the methanol level based on the time an ultrasonic wave takes to propagate through the methanol solution as well as sensing the temperature.

2.6 Temperature measurement

In order to measure ambient temperature there are several methods available for interfacing 1-WireTM devices such as the DS18B20, DS18S20 or DS1822 (Manufactured by Maxim Technologies) to a micro controller. These methods range from simple software solutions, to using a Serial Interface chip such as the DS2480, to incorporating Dallas Semiconductor's VHDL 1-WireTM Master Controller in a custom ASIC. Ambient temperature is measured as a control measure for the liquid temperature measurement.

The block diagram in Figure 13 illustrates the simplicity of the hardware configuration when using multiple 1-WireTM temperature sensors. A single-wire bus provides both communication access and power to all devices. Power to the bus is provided through the 4.7K pull-up resistor from a 3 V to 5.5 V supply rail. An almost unlimited number of 1-WireTM devices can be connected to the bus because each device has a unique 64-bit ROM code identifier.

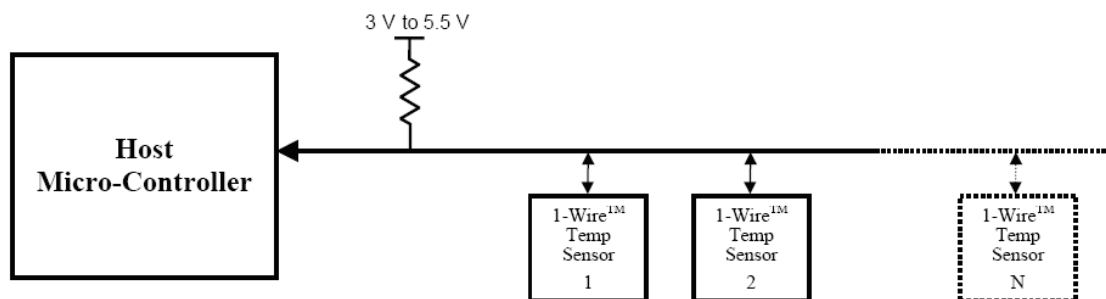


Figure 13: Typical configuration for the DS18X20 temperature sensors

2.7 Flow control

To discuss flow control it is important to know that there are many types of pumps available on the market by taking into consideration the type of flow rate needed for DMFCs which should be in the order of 0.05 to 0.1 L min^{-1} . It is also important to note that the pump used must not consume all the power generated by the fuel cell.

2.7.1 Dosing Pumps

All pumps are classified according to the pumping mechanics involved. Some defined by Liquid Metering Instruments Limited are Air Operated Diaphragm, Electric Drum Transfer, High Pressure Metering, Magnetic Coupled Seal-Less, Motor Driven Metering, Peristaltic, Solenoid Driven Metering.

KNF micro diaphragm liquid pumps are based on the principle of the oscillating displacement pump which is remarkably simple in design. The circular power from the motor is converted into vertical movement by an eccentric axis. This motion is then transferred to a diaphragm by means of a connecting rod which in conjunction with an inlet and outlet valve creates a pumping action.

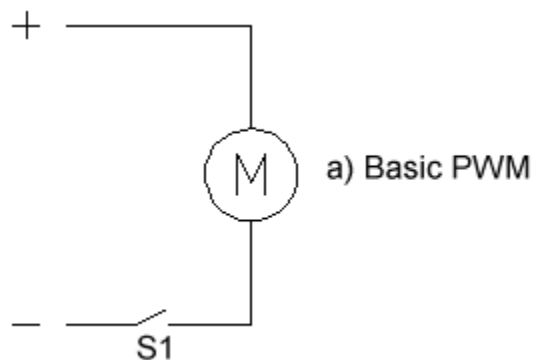
The NF 10/11 type liquid pumps can be mounted in any position and can deliver up to 0.1 L min^{-1} depending on the model and will operate against pressures of up to 10 mWg. The KNF modular system contains a wide standard range of materials, motors, voltages and frequencies to enable the selection of an optimal solution. Annexure B gives more information on these pumps.

The use of chemically resistant materials such as PTFE, PVDF, FFPM or other material combinations for the parts which come in contact with the liquid allows almost all neutral or corrosive liquids to be pumped.

2.7.2 Motor and pump speed control

Lawrence (<http://www.webelectricproducts.com>) states that in the basic Pulse Width Modulation (PWM) method, a switch is turned on and off to modulate the current to the motor. The ratio of 'on' time to 'off' time is what determines the speed of the motor. As an example, if the switch is on for 1 ms and off for 9ms, the ratio is 1 out of 10, or 10%. Another way to express this is having a duty cycle of 10%. There are many ICs available that will do this.

But these two methods only allow the motor to go in one direction. If the motor has to run both forward and in reverse, you need to set up a circuit that allows you to reverse the polarity of the motor (Figure 14). This is called an **H bridge**.



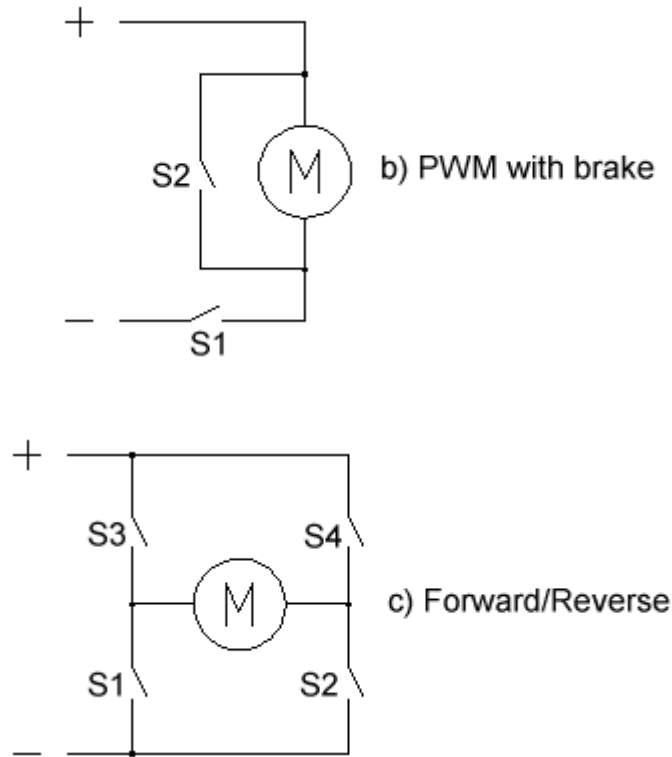


Figure 14: Pulse width modulation setup

If switches S3 and S2 are closed, the motor will spin in one direction, and if one of these switches is modulated, the speed can be controlled. If switches S4 and S1 are closed, the motor will spin in the other direction, and the speed can be controlled by modulating one of these switches. Also note that in this configuration, if switches S1 and S2 are closed it can cause the motor to brake as in the circuit above. For the purpose of this research the basic PWM method will be used in order to control the flow rate of the methanol.

2.8 Summary

This chapter considered the history of fuel cells and the theory of operation of a methanol fuel cell. Different methods of sensing concentration were described as well as the electronic measurement of temperature. Dosing pumps and the control of pump speed were discussed.

The next chapter discusses a design of a practical methanol concentration controller and the algorithms needed for the design. The mathematical models needed for temperature measurement and detector voltage measurement will also be considered.

Chapter 3 Design of a DMFC concentration controller

3.1 Introduction

The previous chapter considered the operation of a DMFC together with the parts needed to build a methanol concentration controller. Aspects like temperature measurement, dosing pumps and different sensing methods were considered.

This chapter will focus on the layout and design of a methanol concentration controller together with the calibration needed to design such a controller. Finally the design considerations will be discussed.

3.2 Concentration controller assembly

The complete design of a methanol concentration controller will evolve around the sensor used to determine the concentration mix of methanol and pure water. The very first step thus was to determine what type of sensor could be used in the design of the controller.

As mentioned in Chapter 2 there are several methods developed for measuring the concentration of methanol. These include:

- Methods using a Böhme meter and dielectric constant
- pH measurement
- Conductivity measurement
- Methods adopting infrared absorption and refraction factor
- Ultrasonic methods

The ultrasonic method was found to be suitable for measurement, as this method is non-invasive and offers real-time measurement. Sound velocity in a methanol solution varies with the concentration of the methanol and the temperature of the solution (Asada 2006:34).

There are a number of ways to determine which of the parameters change when water and methanol are mixed. One of the first considerations was to test what happens to the pH of the concentration of water and methanol mixture. A laboratory electronic pH measuring instrument was used. Two tests were conducted. One on pure water where the pH measured was around 7 and in the second with a mixture of 50% methanol the change was hardly noticeable. This method for testing concentration was then not considered as an option for the control system. The second method used to test concentration was to test the conductivity of the mixed liquid

compared to that of the pure water and again it was not found to be a feasible method for the testing of the liquid because the change in concentration was not clearly noticeable.

The next possible solution was to find a commercial sensor and only two types were found. The first is manufactured by Texas Instruments for Sensata Technologies and the second by Murata Manufacturing Co. Ltd. Sensata Technologies methanol concentration sensor is an optical sensing device for real time methanol concentration analysis. This sensor is a miniaturized, self-contained optical system; shown in Figure 15, which measures the refractive index of aqueous methanol samples rapidly and affordably. The patented sensor design enables in-line process control for methanol-based fuel systems.

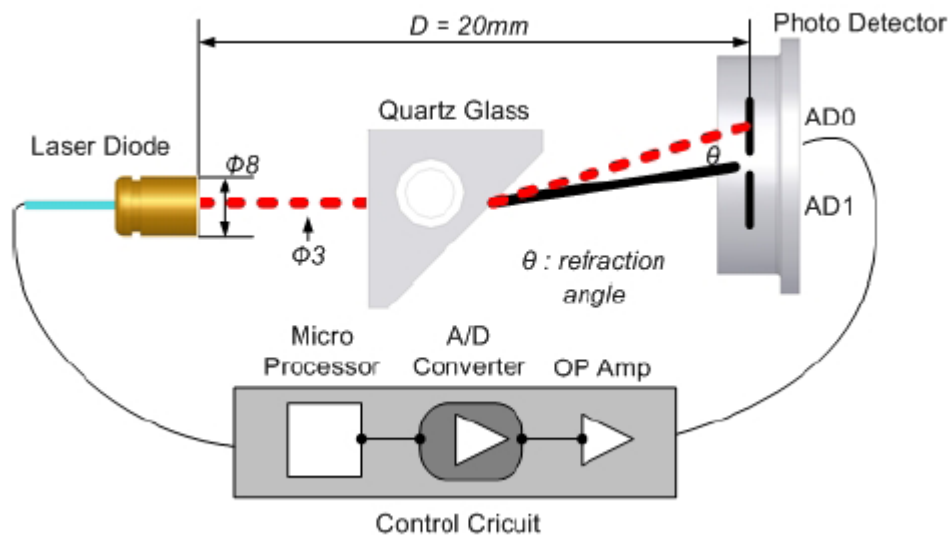


Figure 15: Experimental set-up for optical sensing system (Sung Min Cho et al.)

This sensing system resolves extremely small changes in concentration, in the order of 0.01%, while providing a large dynamic measurement range (0~100% methanol concentration). The above sensor seemed to be ideal but the manufacturer, Texas Instruments, did not want to supply this sensor as it was only manufactured for the exclusive use of Sensata Technologies.

The second manufacturer, Murata Manufacturing Co. Ltd, has introduced an ultrasonic impulse transducer based on a laminated piezoelectric ceramic technology.

This sensor is based on the fact that sound velocity in a methanol solution depends on the concentration of the methanol and the temperature of the solution. In fact, within the thin concentration range of several percent, a change of 1 percent in the concentration of methanol results in a change of 3.4 ms^{-1} in the sound velocity according to Takaaki Asada, Chief of the

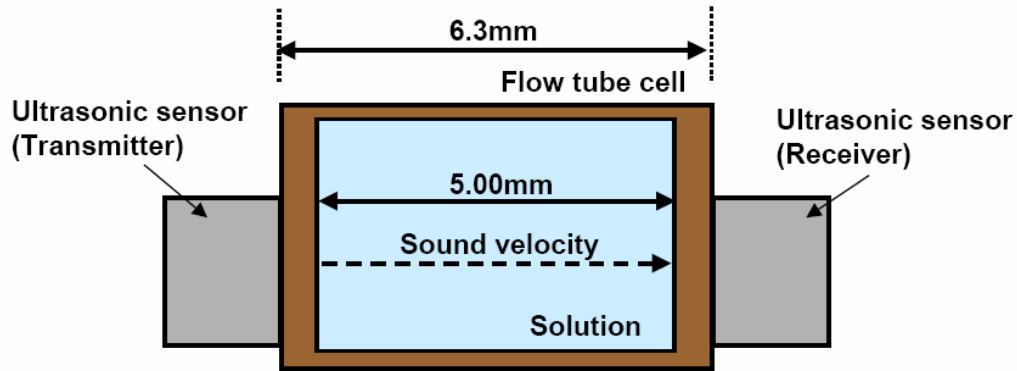


Figure 16: Acoustic configuration of the sensor (Murata Manufacturing Co. Ltd)

When the methanol has a concentration of 2 to 5 percent at 25°C, a change of 1 percent in concentration produces a change of 3.4 m/s in sound velocity. Figure 16 illustrates a basic configuration of the acoustic system of the sensor. To be able to measure sound velocity with high precision, the time with which an ultrasonic wave radiated by the ultrasonic transmission transducer takes before attaining the ultrasonic reception transducer located at a definite distance must be determined precisely.

Figure 17 shows an ultrasonic transmission impulse transducer and an ultrasonic reception impulse transducer which are bonded on both sides of the resin rectangular tube. The transducers are facing each other with a methanol and water solution and the resin tube in between. The printed circuit board with the drive control IC and other devices mounted are bonded on the top surface of the tube to constitute a sensor module.

The methanol solution to be measured is fed through the rectangular tube and the delay time between the transducers is measured to determine the sound velocity. The ultrasonic wave pulses radiated by the echo sounder transmitter passes through the resin diaphragm, the measuring methanol solution and the opposite resin diaphragm, and are received by the echo sounder receiver. The dedicated IC generates pulse signals for driving the echo sounder transmitter and converts the timing difference between the zero-cross of the transmitted signal and that of the received signal into direct-current signals. These direct-current signals are used to determine the propagation velocity of sound waves in the solution. Rectangular pulses with a pulse width of 83 ns in pulse width and 5 V_{p-p} voltages are applied to the transmission transducer.

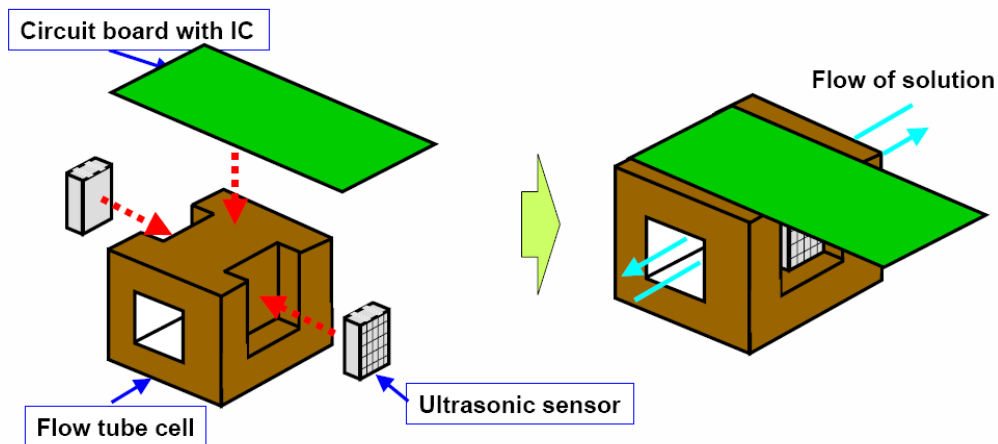


Figure 17: General view of the sensor (Murata Manufacturing Co. Ltd)

Figure 18 shows the terminal voltages of the transmission transducer and the reception transducer. A single ultrasonic sinusoidal impulse measurement range indicated minute changes in the solution concentration in the order of 1 percent should be clearly sensed. The change in sound velocity in relation to the methanol concentration depends on the concentration range of methanol and the temperature of the solution. When the methanol has a concentration of 2 to 5 percent at 25°C, a change of 1 percent in concentration produces a change of 3.4 ms^{-1} in sound velocity.

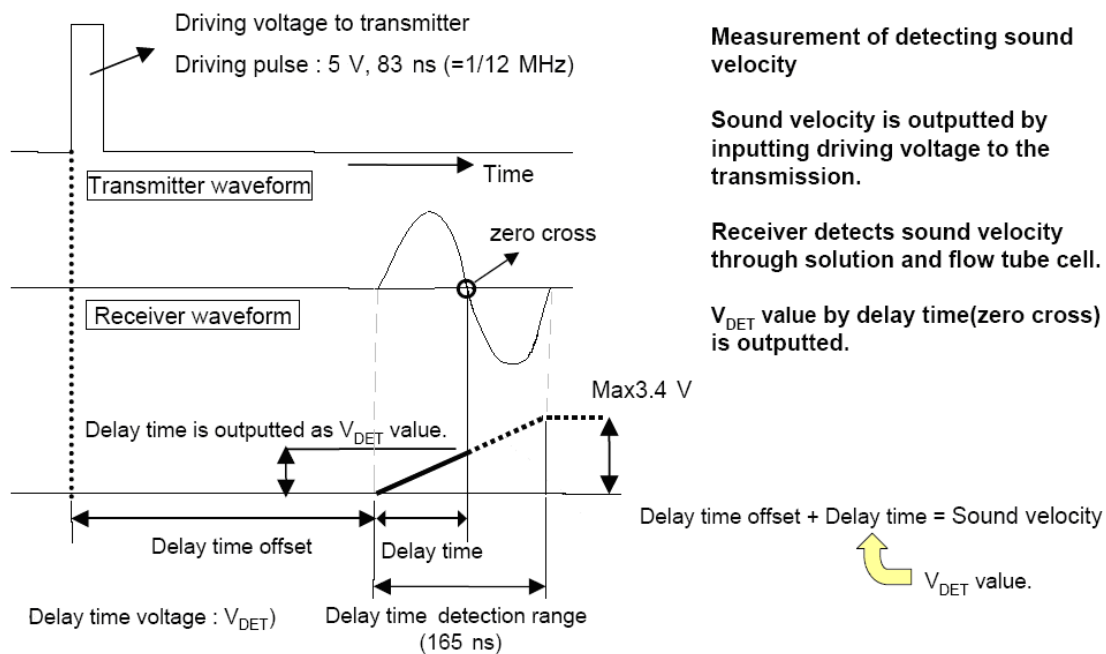


Figure 18: Driving signal voltage and received sound pressure (Murata Manufacturing Co Ltd)

The other main advantage of this sensor is that it has a built-in sensor for temperature measurement. Therefore this sensor was chosen for this design.

3.3 The electronic design

The electronic design of the methanol controller was made after selecting all the necessary components needed. A PIC micro controller was used together with the Murata sensor. The design consists out of two parts namely the software design and a hardware design.

Figure 19 shows the basic flow diagram for the micro controller software program used in the methanol controller system.

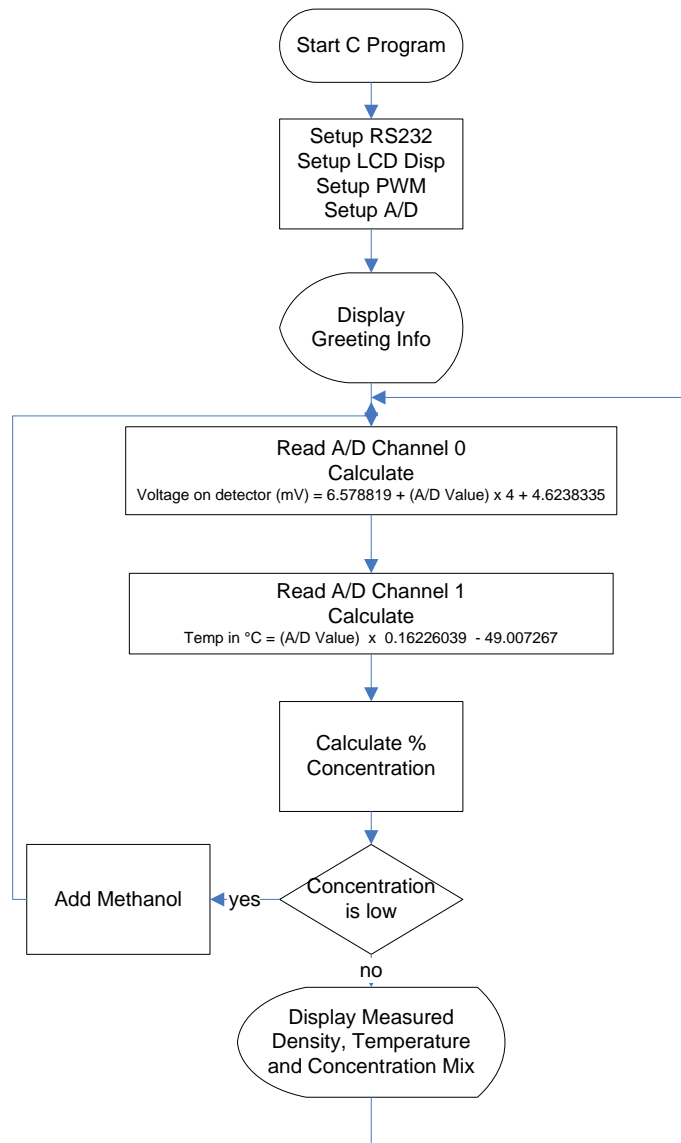


Figure 19: Flow diagram of the methanol controller software

After the setup and greeting phase it measures and converts the detector voltage and also calculates the correct detector voltage. The temperature is measured and calculated next. Then the algorithm (See equation no 6 on p.36) is applied to determine the volume of methanol in the solution being tested.

The second part, the hardware design was done using the following components: The Murata Sensor with a PIC 18F452 micro controller. For the speed control of the pump a L6202 H-Bridge IC was used and a MAX232 Serial controller was used for the data logger.

The second most important device after selecting the sensing device would be the micro controller and there were plenty to choose from. The device selected for this design was a PIC 18F452 since it was readily available and it contained all the needed functions like analogue to digital conversion, pulse width control and a built-in serial port. Figure 20 shows the block diagram of the designed concentration tester.

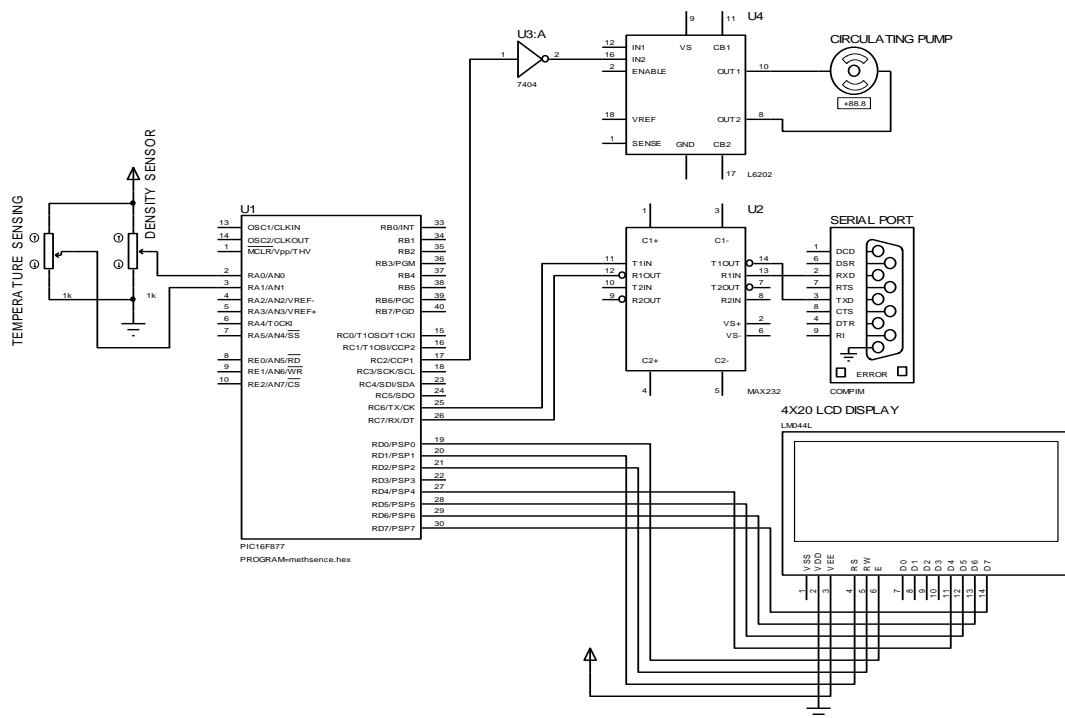


Figure 20: Basic layout of the methanol concentration tester

The circulating pump which is used to pump the solution through the sensor (See Annexure B) is connected to an H-Bridge (L6202 situated at the right-hand topside of the circuit) which is needed for the supply of the circulating pump and the speed control thereof. The H-Bridge is connected to an inverter and the output of the pulse width modulator of the PIC micro controller. The pulse

width modulator is used to vary the speed of the circulating pump. The aim of this part of the design is to test the influence of changing the flow rate, on the sensor.

A 4 line LCD display (bottom right in Figure 20) is used to display the outputs measured from the ultrasonic detector and the temperature sensor. It shows the calibrated values measured for the detector voltage, temperature of the fuel, the air temperature and the volume mix percentage. It also shows when methanol is added and if the temperature is changing too fast for accurate measurement.

To enable data logging on a PC a MAX232 (middle right in Figure 20) is added to the circuit, which enables recording on a PC of all measured values. Furthermore the Murata sensor (middle left in Figure 20) was added to channel 1 (concentration) and 2 (temperature) of the analogue converter of the micro controller. A button connected to the microcontroller allows for changing the volume mix of the concentration.

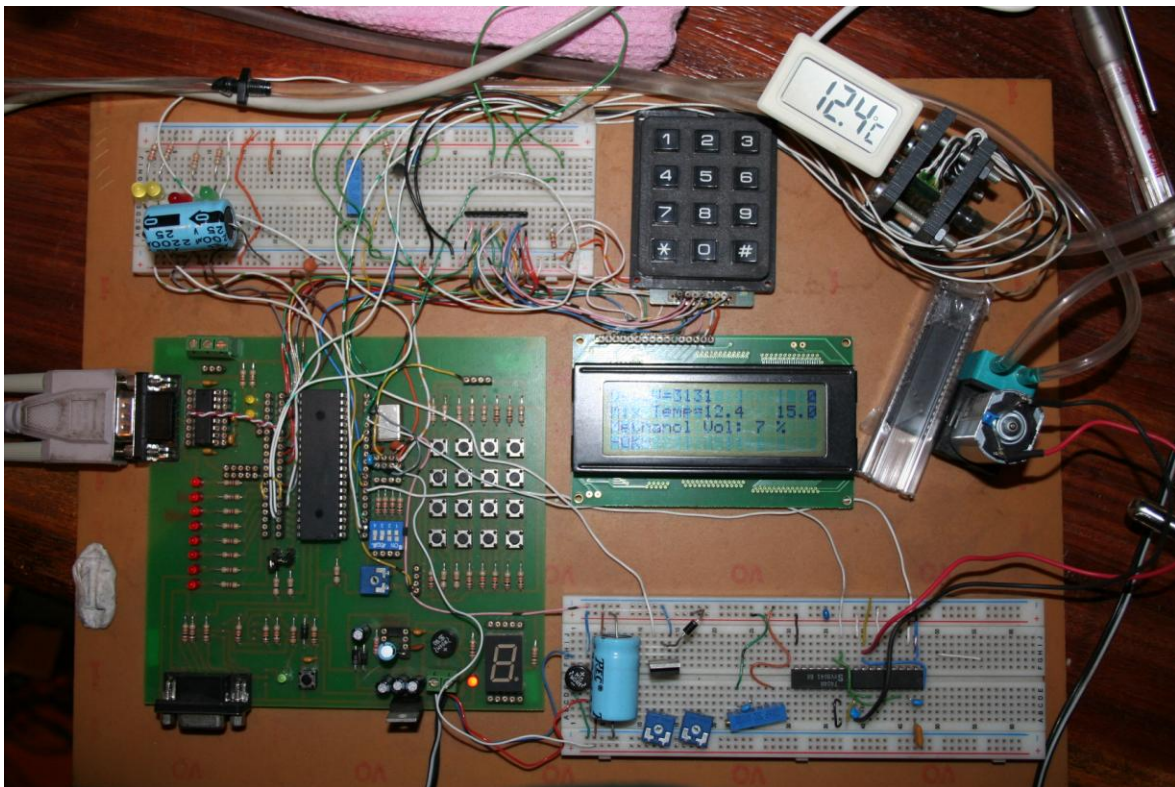


Figure 21: Layout of the prototype

3.4 Summary

In this chapter the basic concepts of the design were discussed and also the reason for choosing the Murata sensor for detecting the concentration levels. In the next section the results obtained from the measurements will be discussed together with the calibration methods followed.

Chapter 4 Measurements and Results

4.1 Introduction

The previous chapter presented the design of the methanol concentration tester and the electronic circuit model for the tester. The reason for choosing the Murata ultrasonic detector was also given. The first test on this circuit was to perform temperature calibration of the built-in temperature sensor. Using the same circuit, samples were taken starting from 0% up to 10% with 2% intervals while slowly changing the temperature from 20° to about 60° Celsius. The same test was done with 4 other samples using 4% methanol to water mix to test the stability of the measurements. The last test conducted was to change the flow rate a little bit every second and keeping the temperature at room temperature to see if the flow rate would have any effect on the measurements obtained.

4.2 Temperature calibration

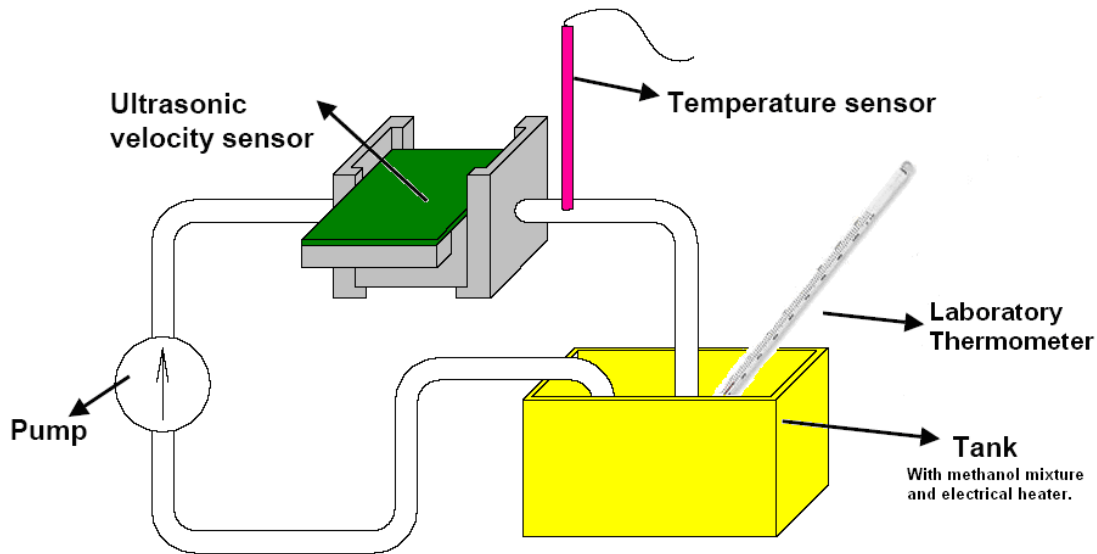


Figure 22: Basic layout of the sensor liquid circuit

Figure 22 shows the liquid path diagram of the concentration tester. The tank that was used was made of high thermal plastic, which could easily be heated up in a warm bath to ensure measurements at different temperatures. An electric heater connected to a thermo controller was used as the heating bath to ensure the gradual heating up of the methanol mixture while circulating the mixture through the sensor.

The first test was done obtaining values from the analogue to digital converter on the temperature sensor. These readings were compared with the readings obtained from a laboratory thermometer. Care had to be taken to make sure that the sensor was ready to display the correct temperature since it normally takes a few seconds to adjust to temperature changes. The temperature of pure water was measured as the temperature was very slowly increased. The following results were obtained:

Table 1: Calibration Values for temperature

A/D Value	Temp measurement in °C
427	19.3
518	36
543	40
577	45
610	48.8
626	53
645	55.5
663	58.2

After analysing the above data and testing quadratic as well as linear equations, the best fit for the measurements was found to be a linear equation as shown in Figure 23:

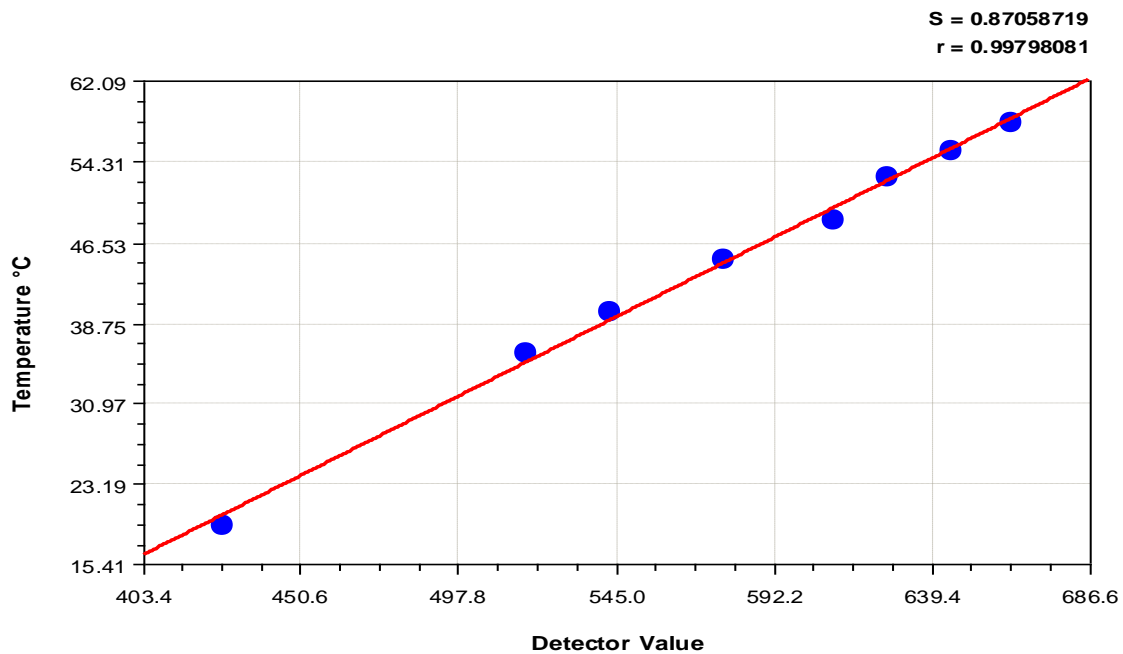


Figure 23: Measurement of temperature against A/D values obtained from the detector

Figure 23 shows the values obtained from the ADC (Analogue to digital converter) compared with temperature measurements on a linear fitted graph. The derived linear expression for the calibration of the temperature values measured versus the ADC values was as follows:

$$y = a + bx$$

The coefficient data were calculated as follows:

$$y = -49.007267 + 0.16226039x \quad (3)$$

To determine the correct temperature value from the ADC value the following formula was used:

$$\text{Temp in } ^\circ\text{C} = (\text{A/D Value}) \times 0.16226039 - 49.007267 \quad (4)$$

4.3 The detector voltage calibration

To determine the correct detector voltage the same procedure was followed as above. ADC values obtained from the ultrasonic detector were compared with a laboratory multimeter's voltage readings. The following measurements as shown in Table 2 were obtained:

Table 2: Voltage values measured on detector versus A/D values read by the microprocessor

ADC Value	Voltage Measured mV	ADC Value	Voltage Measured mV
345	1610	550	2540
354	1651	560	2590
360	1669	570	2640
370	1723	580	2680
380	1765	590	2740
390	1813	603	2800
400	1860	610	2830
410	1902	620	2880
421	1954	634	2950
430	2000	640	2970
441	2040	650	3020
450	2090	664	3080
460	2130	670	3110
470	2180	680	3140
480	2220	690	3200
490	2270	700	3240
500	2310	710	3290
511	2360	720	3340
520	2400	730	3380
532	2460	740	3430
540	2500		

Displaying the data graphically again the equation was found to be linear as was the case with the temperature measurements.

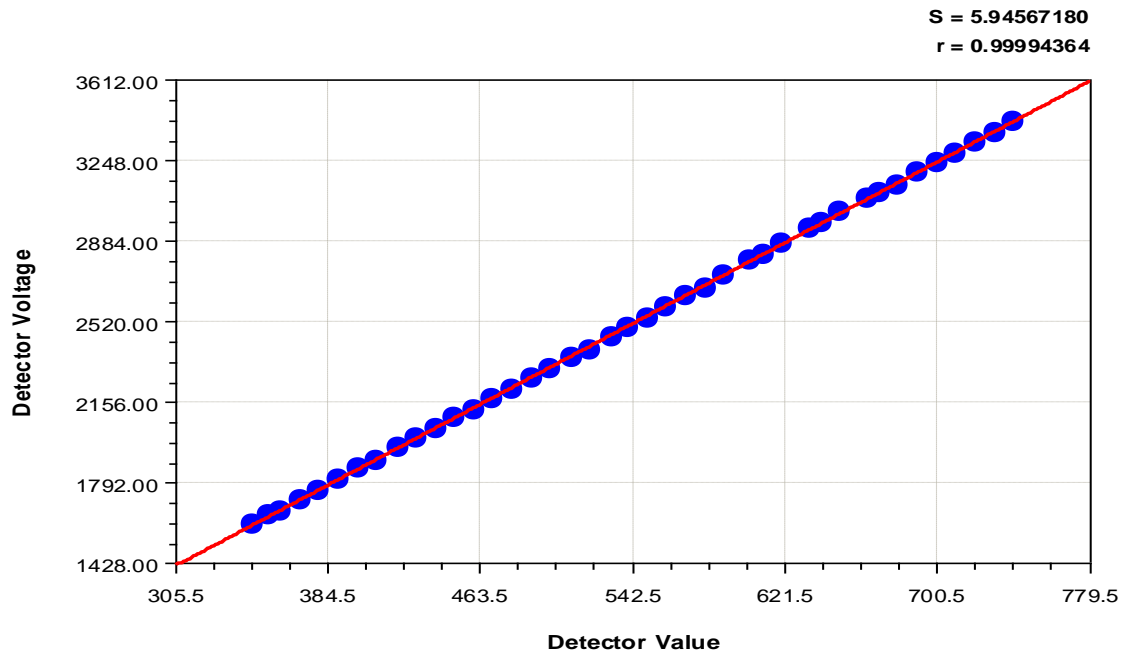


Figure 24: Voltage values measured on ultrasonic detector versus A/D values read by the microprocessor

The equation is given by:

$$\text{Voltage on detector (mV)} = 6.578819 + (\text{ADC Value}) \times 4.6238335 \quad (5)$$

4.4 Temperature effects on the detector

The following properties of pure water were also used:

- At 4°C pure water has a density (weight or mass) of about 1 g cu.cm⁻¹ or 1 g ml⁻¹.
- At 4°C pure water has a specific gravity of 1.

Since the Murata sensor used in this design is sending ultrasonic pulses through the concentration it can be concluded that the sensor actually measures the density of the liquid. Looking at the density table obtained from Simetric we can see that the temperature will have an effect on the density. According to Simetric the density of pure water is a constant at a particular temperature, and does not depend on the size of the sample. The density of water also varies with temperature and impurities.

Table 3: Density table of water (Simetric)

Temp (°C)	Density pure water (g cm ⁻³)	Density tap water (g cm ⁻³)	Specific Gravity 4°C reference
0 (solid)	0.915	-	0.915
0 (liquid)	0.9999	0.99987	0.999
4	1	0.99999	1
20	0.9982	0.99823	0.998
40	0.9922	0.99225	0.992
60	0.9832	0.98389	0.983
80	0.9718	0.97487	0.972
100 (gas)	0.0006		

Using the above data and using a statistical curve-fitting algorithm the graph in Figure 25 displays how density changes with temperature.

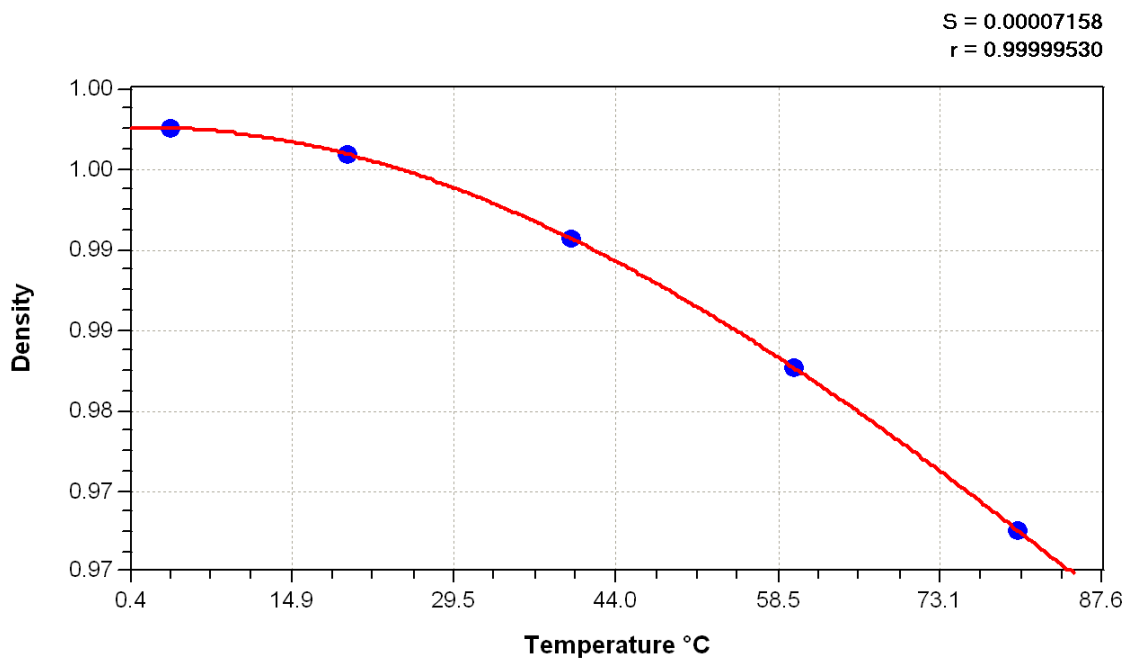


Figure 25: Density versus temperature of pure water

The algorithm used is a 3rd degree polynomial fit and is given by:

$$y = a + bx + cx^2 + dx^3$$

Coefficient Data:

$$y = 1.0000145 + 2.3778903e-005x - 6.1901133e-006x^2 + 1.8569977e-008x^3$$

(6)

It was therefore important to test the effects of temperature changes on the detector. Testing heating up and cooling down of pure water gave the following results as shown in Figure 26:

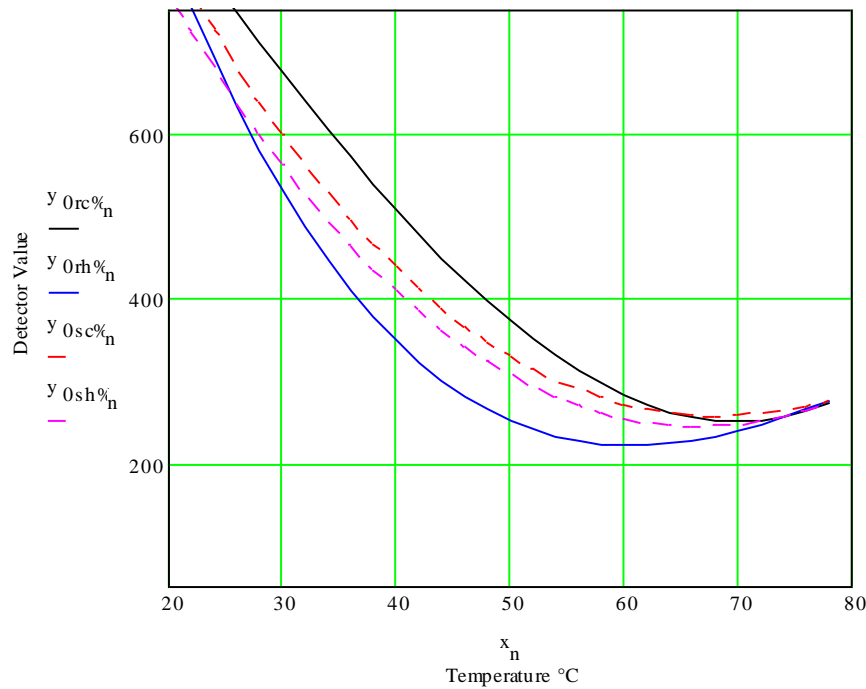


Figure 26: Detector values versus temperature of pure water

Figure 26 shows the heating up and cooling down curves of pure water. The curves $y_{0rc\%}$ and $y_{0rh\%}$ shows the effect of a quick cool down and heat up of the water respectively. The curves $y_{0sc\%}$ and $y_{0sh\%}$ shows what happens to the detector value if the water is cooled down and heated up slowly. The slow cool down results were obtained by leaving the concentration tank in about 5l of water and letting the water cool down by itself to ambient temperature. The slow heating up of the tank was done by heating up the concentration tank in the same 5l of water. The temperature was adjusted by 5°C at a time and then waiting for the detector values to stabilize for at least 10 readings of the same temperature reading, taken 1 second apart. Values were then recorded by the data logger for approx. 1 minute at this time.

From these results it was concluded that the temperature detector built into the sensor is slow to react and care had be taken to ensure correct reading of the ultrasonic detector at the right

temperature. This was proven further by looking at the high end of the temperature curve when the rapid heating effect is starting to slow down. It seemed that the best results could be obtained from a slow cool down test since the heat up curve could have minor discrepancies since the stabilisation might not have taken place as needed. The problem however is that with a methanol mixture, the methanol starts to vaporise at round about 63°C and therefore all further testing was performed up to a max. of 60°C.

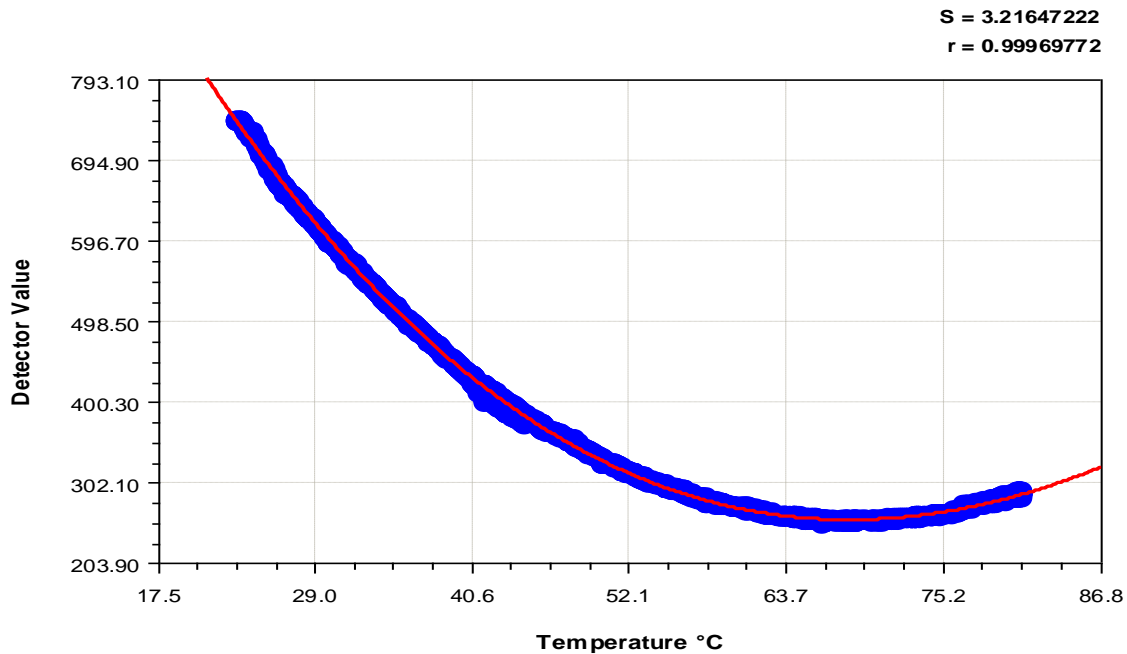


Figure 27: Detector values versus temperature of pure water on a slow cool down test

During the slow 0% mix cool down test the thermocouple of the heater tank was set at 40°C and left in that position for about an hour. Every time the heating element came on the water was heated up to about 43°C and then cooled down to 40°C. From Figure 27 it can be seen that the readings obtained from the detector shows a slight change in the density of the curve between 40°C and 43°C. This again proves that special care had to be taken to ensure correct temperature readings. The mathematical best fit for the curve is a 3rd degree Polynomial Fit of equation 4 and the following coefficient data:

$$y = 1459.6325 - 39.009631x + 0.36916464x^2 - 0.00081497268x^3 \quad (7)$$

4.5 Testing stability of the detector

To test the stability of the detector a 4% volume mix of methanol and water was tested using the cool down method and using the same solution 8 hours apart. A 4th test ($y_{4ss\%n}$) was done with a new liquid mix and using a very slow cool down period.

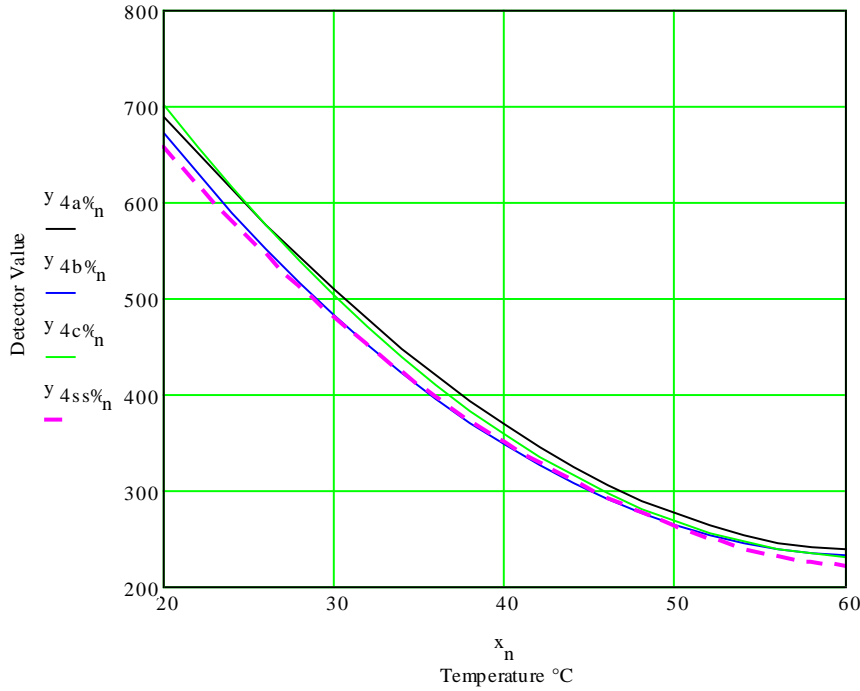


Figure 28: 4% by volume methanol mix on a slow cool down test repeated 3 times

From Figure 28 the black line shows the first test and the compared values of two more tests on the same solution. The dashed red line was done with a new liquid mix. Again from the above test it can be seen that the temperature readings are very critical in this test. The mathematical 3rd degree polynomial equations of the 4 curves were different every time. It can also be noted here that the 3rd degree value is very small and can be omitted for further calculations and thus quadratic functions will be used further. The equations are given by:

$$\begin{aligned}
 y_{4\%a_n} &= 1134.761 - 24.2148 \times temp + 0.071312 \times temp^2 + 0.001390944 \times temp^3 \\
 y_{4\%b_n} &= 1212.607 - 32.3762 \times temp + 0.269971 \times temp^2 - 3.86 \times 10^{-5} \times temp^3 \\
 y_{4\%c_n} &= 1253.940 - 32.6614 \times temp + 0.250094 \times temp^2 + 0.00017402 \times temp^3 \\
 y_{4\%d_n} &= 1142.311 - 28.6959 \times temp + 0.223025 \times temp^2 - 1.69 \times 10^{-5} \times temp^3
 \end{aligned}
 \tag{8}$$

Another test done to ensure the correctness of the values read was to vary the speed of the circulating pump to see if this would have an effect on the values measured. As can be seen from Figure 29 the fluctuations measured were only a few milli-volts. The temperature was held as constant as possible over this period and the minor changes in detector voltage could have been caused by minor temperature changes. The maximum deviation measured here was not more than 14 mV and this will have little effect on the control of the methanol concentration as the difference between 3% to 4% concentration at 20 °C is in the order of 230 mV.

Figure 30 were obtained at a temperature of 11.6°C. As can be seen from these results, the change with increase in methanol volume is linear with respect to the change in detector voltage. It was also found that the slope of the linearity and the position of the curve changed with increase in temperature as illustrated in Figure 31.

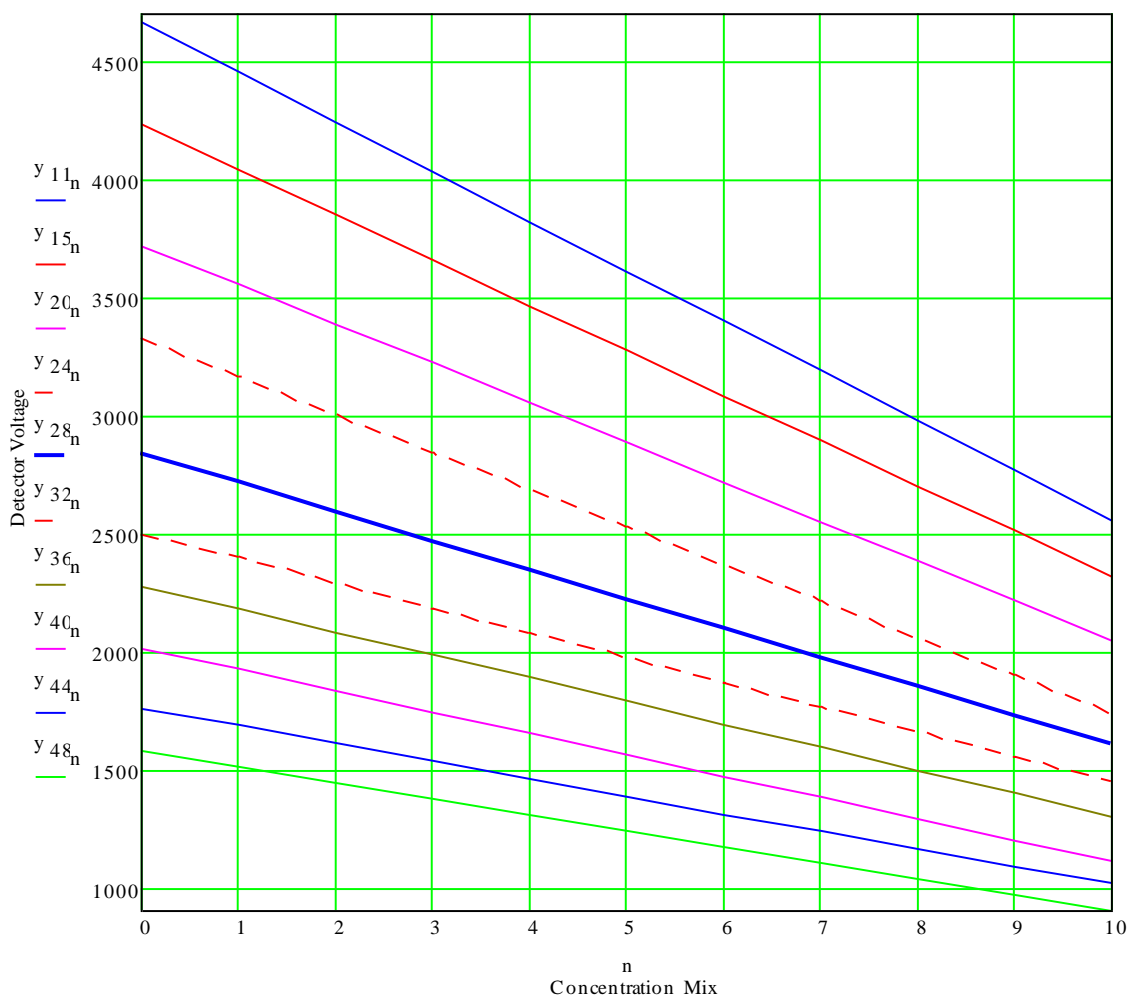


Figure 31: Varying circulation speed readings to test stability

The data was collected at temperatures 11.6, 15.72, 19.8, 23.88, 27.96, 32.04, 36.12, 40.2, 44.29, 48.37 °C respectively. The collected data were used to derive linear equations to fill in the values for the odd numbered concentration mixes which produced the following data table. The values in table are the ADC values for temperature and detector voltages. For the sake of accuracy all the calculations were done using the ADC values rather than the derived temperature and detector voltages.

Table 4: Temperature comparison table

Temp in C	0%		1%		2%		3%		4%		5%	
11.6	375	1008	375	962	375	916	375	871	375	825	375	779
15.72	400	914	400	872	400	831	400	790	400	748	400	707
19.8	425	803	425	767	425	731	425	695	425	659	425	622
23.88	450	717	450	683	450	648	450	614	450	580	450	546
27.96	475	611	475	585	475	558	475	531	475	505	475	478
32.04	500	539	500	517	500	494	500	471	500	449	500	426
36.12	525	491	525	470	525	449	525	428	525	407	525	386
40.2	550	434	550	415	550	395	550	375	550	356	550	336
44.29	575	379	575	363	575	347	575	331	575	314	575	298
48.37	600	340	600	325	600	310	600	296	600	281	600	267

Temp in C	6%		7%		8%		9%		10%	
11.6	375	734	375	688	375	643	375	597	375	551
15.72	400	665	400	624	400	583	400	541	400	500
19.8	425	586	425	550	425	514	425	477	425	441
23.88	450	511	450	477	450	443	450	409	450	374
27.96	475	451	475	425	475	398	475	371	475	345
32.04	500	403	500	380	500	358	500	335	500	312
36.12	525	364	525	343	525	322	525	301	525	280
40.2	550	317	550	297	550	278	550	258	550	239
44.29	575	282	575	266	575	250	575	234	575	218
48.37	600	252	600	238	600	223	600	208	600	193

After the above data was compiled the parabolic equations for each concentration mix were determined. Parabolic equations were used (see next paragraph) since the third degree polynomial values were extremely small.

4.7 Comparing concentration mixes of the detector

After the micro controller was reprogrammed with the parabolic formulas below, the controller was tested with different samples of methanol mix while slowly changing the temperature from 20° to about 60° C. The tests were done in a closed system with 100 ml of fluid to avoid the loss of methanol when the fluid is heated up. The controller successfully tested the different samples but great care had to be taken with fast changing temperature values. The equations for the different solutions were as follows:

$$\begin{aligned}
Det_V_{0\%_n} &= 3742.54 - 10.041 \times temp_val + 0.00728 \times temp_val^2 \\
Det_V_{1\%_n} &= 3546.59 - 9.485 \times temp_val + 0.00685 \times temp_val^2 \\
Det_V_{2\%_n} &= 3494.70 - 9.497 \times temp_val + 0.00698 \times temp_val^2 \\
Det_V_{3\%_n} &= 3209.02 - 8.596 \times temp_val + 0.00623 \times temp_val^2 \\
Det_V_{4\%_n} &= 3010.98 - 8.029 \times temp_val + 0.00579 \times temp_val^2 \\
Det_V_{5\%_n} &= 2839.96 - 7.578 \times temp_val + 0.00548 \times temp_val^2 \\
Det_V_{6\%_n} &= 2672.96 - 7.142 \times temp_val + 0.00518 \times temp_val^2 \\
Det_V_{7\%_n} &= 2495.81 - 6.664 \times temp_val + 0.00483 \times temp_val^2 \\
Det_V_{8\%_n} &= 2318.65 - 6.182 \times temp_val + 0.00448 \times temp_val^2 \\
Det_V_{9\%_n} &= 2136.39 - 5.685 \times temp_val + 0.00412 \times temp_val^2 \\
Det_V_{10\%_n} &= 1979.36 - 5.268 \times temp_val + 0.00382 \times temp_val^2
\end{aligned} \tag{9}$$

Comparing the ADC Value with the derived value will give an indication if replenishment of methanol is needed and this function was also added to the control system. This means that methanol can automatically be replenished with a dosing pump controlled from the micro controller, if needed. The level per volume of methanol needed can also be changed by just pushing and holding the button down.



Figure 32: LCD display of the prototype

Figure 32 shows the display of the prototype indicating on the first line the detector voltage measured. The second line shows firstly the temperature of the methanol mixture and secondly the ambient temperature. The third line indicates the % of the methanol mixture and the fourth line shows different error messages that may be needed to display any errors.

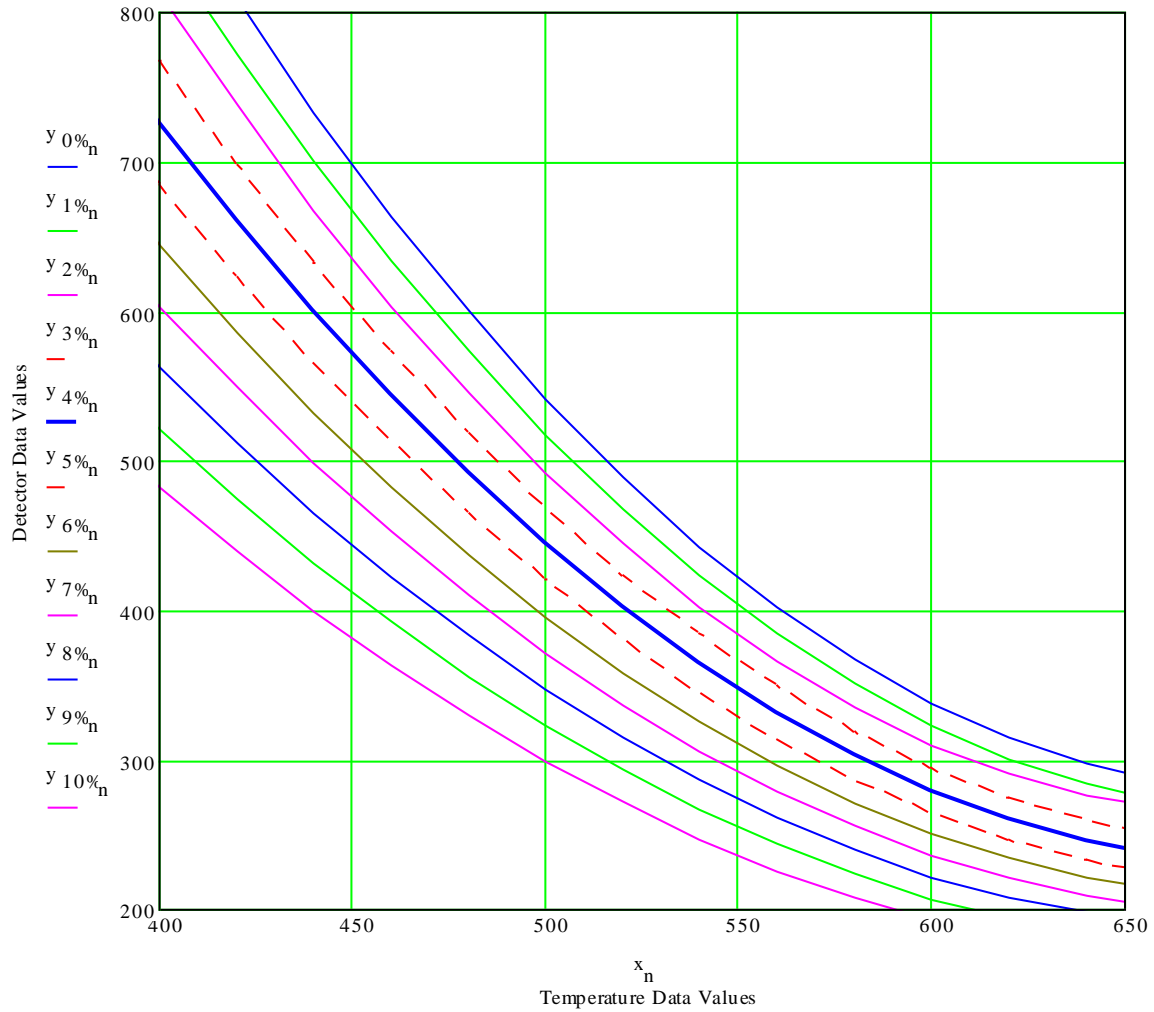


Figure 33: Comparison of different water methanol mix samples changing temperature over time

4.8 Summary

This chapter considered the results of the measurements taken of the methanol controller and how the controller was calibrated. Different methods of calibration were tried but only the methods which proved successful were mentioned in this chapter. The design successfully tested different samples of methanol mixture and indicated correctly the % of methanol.

Chapter 5 is the final chapter in this document. It will conclude this research and discuss recommendations that have evolved.

Chapter 5 Conclusion and Recommendations

5.1 Concluding comments

This chapter presents the conclusions reached with regard to the design of the methanol concentration controller. The initial objectives will be compared with the outcomes of the design. The recommendations for future research will then be used to complete this chapter.

5.2 Conclusions attained from the study

The theoretical study was completed and the most appropriate commercial sensor available for testing density of the concentration mix was found to be the Murata sensor. The Murata sensor makes use of ultrasonic pulses which are propagated through the liquid and the time taken to receive the signal which is then converted into a voltage output and this voltage can then be used as an indication of the density of the fluid. The sensor could easily establish 1% changes in the concentration mix. The sensor also included a temperature sensor which could be utilized for the measurement of the fluid temperature which helps to determine the correct concentration level since temperature plays a major role on the measurements that were taken.

The development and the design of the variable control system were done using a Microchip PIC micro controller 18F452 to control all the functions of the concentration controller. The device was programmed using a PICStart Plus Programmer together with using MPLab programming software. The code was written using the C programming language. The code is displayed in annexure A of this document. The device also has the built-in feature to change the flow rate of the liquid being tested.

A practical design and prototype product of a micro controlled system was build and various measurements were taken to calibrate and to accomplish the design specifications as set out in the objectives of Chapter 1.

Testing the device proved to be successful but great care had to be taken when temperature changed quickly and it is recommended that the container with the fuel cell fuel should be isolated from fast temperature changes. Temperature had a major effect on the calibration of the unit and measurements had to be taken very carefully. It will also be advisable to place the detector as close as possible to the container tank to avoid changing temperatures in the transport system. It was found that when the temperature rises rapidly the detector read higher % than the actual % value and if it cooled down rapidly the opposite is true as can be seen from Figure 26 on p.34 in

the previous chapter. Normally this should not happen since rapid temperature changes should not take place in normal operating conditions.

Methanol can be replenished easily from a methanol tank and a dosing pump connected to the controller. Small spurts of methanol can be added to fuel the fuel cell a couple of seconds apart to ensure replenishment as needed. This should ensure that the methanol is not wasted by crossover. Methanol crossover studies will now be possible with the DMFC control system.

Other tests done with the methanol controller where higher volumes of methanol were used showed some interesting things happening with the methanol density. At between 20% and 30% volume mix the density became inversely affected by the increase in volume. Figure 34 shows how the slope of the graph changes when the volume increases above 30%.

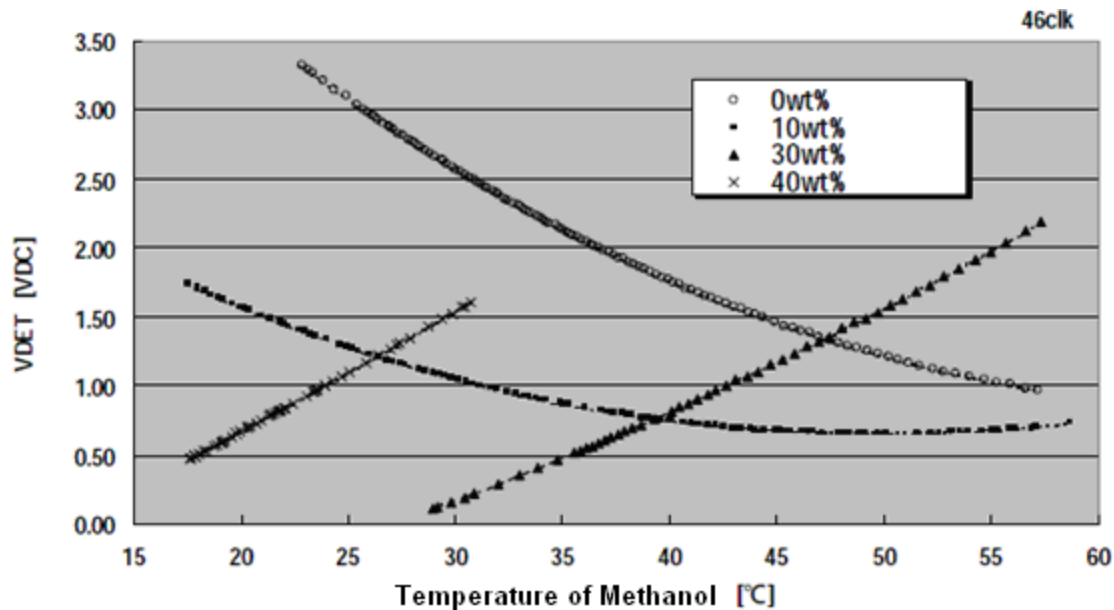


Figure 34: Measurement data of V_{DET} value by temperature and concentration of methanol (Murata Co. Ltd)

When the concentration of methanol is from 0wt% to about 10wt%, sound velocity is proportional to the temperature of methanol. But, when the concentration is more than about 30wt%, sound velocity is inversely proportional to the temperature of the methanol.

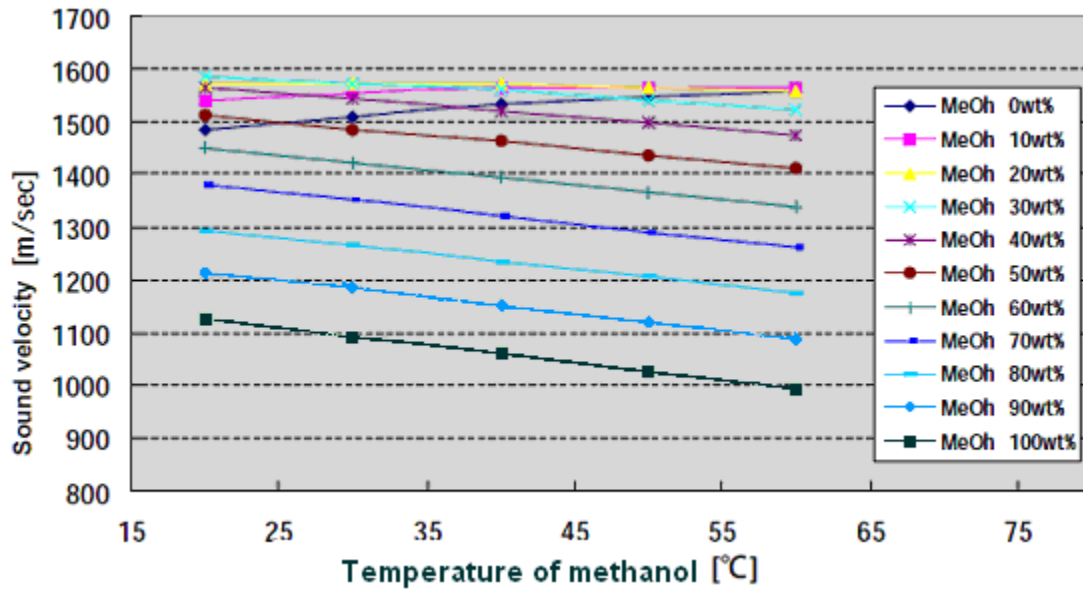


Figure 35: Sound velocity of methanol

From Figure 34 it can be seen that the controller will not work very well if the volume percentage mix is at about 20% to 30%.

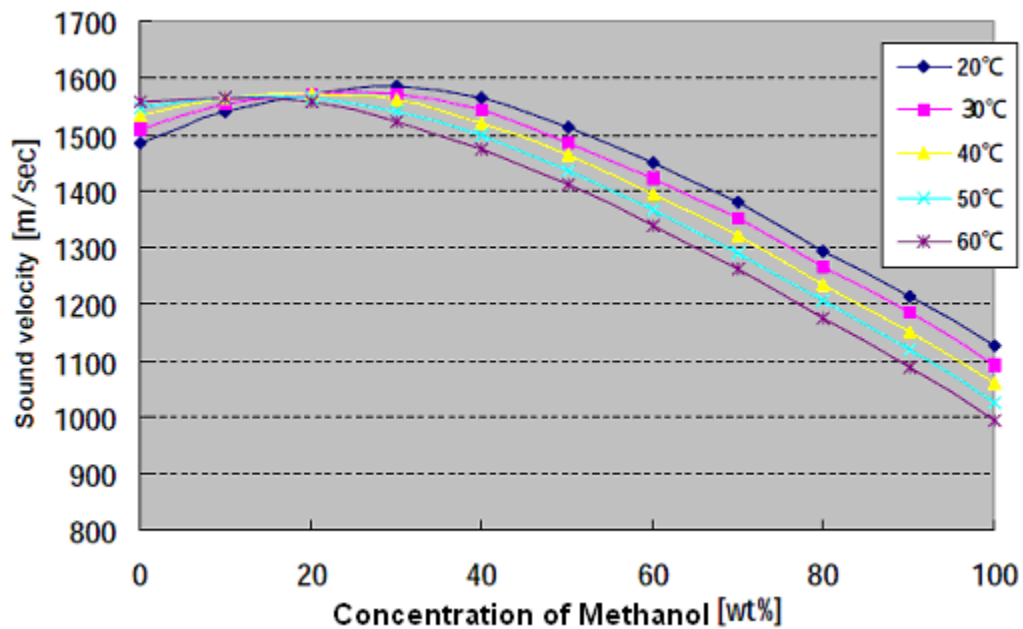


Figure 36: Sound velocity of methanol vs concentration

5.3 Recommendations

The use of an optical detector system should also be investigated as it might produce more rapid and accurate measurements. A more sensitive temperature measuring method can also be considered. This might improve the quality of measurements when the temperature is changing and on startup of the system produce correct readings sooner.

Another option would be to control the concentration of the methanol in the water to adjust for higher or lower currents. In order to do this, the methanol feed should be controlled with current flow out of the fuel cell. This means that methanol should only be added when the load increases. A fuel cell in the regenerative mode can also be considered as a sensor for determining the need of methanol to be added.

5.4 Other applications

The designed controller could also be used for:

- Density testing of other aqueous fluids
- To test for the presence of water in petrol or diesel tanks at filling stations
- Quality of water test in various applications

References

- ACRES, G.J.K. 1973. *Proceedings of 3rd international clean air congress held at Dusseldorf*. 1973. Johnson Matthey PLC.
- ARGYROPOULOS, P., SCOTT, K. & TAAMA, W.M. 2000, *Dynamic response of direct methanol fuel cell under variable load conditions*. Journal of Power Sources 87:153.
- ASADA, T. 2006. *Murata's methanol concentration sensors fuel DMFC use in mobile*. AEI, September 2006. Dempa Publications, Inc.
- AYHAN, A.F. 2002. *Design of a piezoelectrically actuated microvalve for flow control in fuel cells*. Masters Thesis. University of Pittsburgh: School of Engineering.
- DEPARTMENT OF ENERGY. 2002. *Fuel cell handbook*. 6th ed., DE-AM26-99-740575, Morgantown, WV.
- DOHLE, H., DIVISEK, J., MERGEL, J., OETJEN, H.F., ZINGLER, C. & STOLTEN, D. 2002. *Recent developments of the measurement of the methanol permeation in a direct methanol fuel cell*. Journal of Power Sources. 105:313-322. 20 March 2002.
- DTI ENERGY INC. *Uses of DMFC (Direct Methanol Fuel Cell) technology*. [Online]: <<http://www.dtienergy.com/>>. Accessed 15/03/2007.
- FUEL CELL INFO-CD IL. 2008. *Innovations for the building services of the future*.
- GEITMANN, SVEN. 2004. *Wasserstoff und Brennstoffzellen: Die Technik von Morgen*. Hydrogeit Verlag.
- GRIFFITHS, T. *Understanding PH Measurement*. [online] <<http://www.sensorland.com/HowPage037.html>>. Accessed 15/03/07.
- GURAU, J. & SMOTKIN, E.S. 2002. *On-line mass spectrometric analysis of fuel crossover in non-hydrogen fuel cells*. Power Sources 112:339–352.
- HAYNES, C.L., GRAY, G., PAREKH, D., WILLIAMS, A., LEAHY, S. & SPADACCINI, R. 2003. *Development of an 'AC' fuel cell stack via active flow control*, Georgia Tech Research Institute Year-End IRAD report.
- HEINZEL, V.M. & BARRAGAN, J. 1999. *A review of the state-of-the-art of the methanol crossover in direct methanol fuel cells*. Journal of Power Sources 84:70–74.
- HOTZ, N., MING-TSANG, L., GRIGOROPOULOS, C.P., SENN, S.M. & POULIKAKOS D. 2006. *Exegetic analysis of fuel cell micro power plants fed by methanol*. International Journal of Heat and Mass Transfer 49:2397–2411.
- HOGARTH, M. 2003. *Fuel cell technology handbook*. Edited by Gregor Hoogers. CRC Press.
- KNF FLODOS. n.d. *Micro diaphragm liquid pumps data sheet E 511*. Sursee, Switzerland.

- LARMINE, J. & DICKS, A. 2003. *Fuel cell systems explained*. England: John Wiley & Sons.
- LAWRENCE, A. *A microcontroller based motor speed control*. [Online] <<http://www.webelectricproducts.com/01/2/speed1.htm>>. Accessed 15/03/2007.
- LEAHY, S.B. 2004. *Active flow control of lab-scale solid polymer electrolyte fuel cells* Masters Thesis, Atlanta: Georgia Institute of Technology. March 2004.
- METTLER-TOLEDO THORNTON. *Electrical conductivity*. [Online] <<http://www.wileywater.com/TheEncyclopediaofWater.htm>>. Accessed 15/03/2007.
- NARAYANAN, S.R. 2003. *Direct methanol fuel cells: Fundamentals and applications*. Abs. 1095, 204th Meeting, © 2003 The Electrochemical Society.
- NARAYANAN, S.R., VALDEZ, T., WHITACRE, J. & SURAMPUDI, S. 2006. *Direct methanol fuel cells - Progress, problems and prospects*. Pasadena: Jet Propulsion Laboratory, California Institute of Technology.
- NASA.1996. *Making catalysts and electrodes for liquid-feed fuel cells*. (NPO-19893) NASA Tech Briefs, Vol. 20, October: 60.
- NGUYEN, T.V., & YI, J.S. 1999, *Multi-component transport in porous electrodes of proton exchange membrane fuel cells using interdigitated gas distributors*. Journal of the Electrochemical Society, 146(1):38-45.
- NICE, K. *How fuel cells work*. [Online]. Available at: <<http://science.howstuffworks.com/fuel-cell.htm>>. Accessed 15/03/2007.
- PUKRUSHPAN, J.T., STEFANOPOULOU, A. & PENG, H. 2002, *Modeling and control for PEM fuel cell stack systems*. Proceedings of the American Control Conference, pp.3117–3122.
- REN, X. & GOTTESFELD, S. 2001. *Electro-osmotic drag of water in poly(perfluorosulfonic acid) membranes*. Journal of Electrochemical Society 148:A87–A93.
- REN, X., ZELANAY, P., THOMAS, S., DAVEY, J., & GOTTESFELD, S. 2000 *Recent advances in direct methanol fuel cells*. Power Sources 86: November 2000.
- REN, X., SPRINGER, T.E. & GOTTESFELD, S. 2000. *Water and methanol up- takes in nafion membranes and membrane effects on direct methanol cell performance*. J. Electrochemical Society 147(1):92-98.
- ROOKER, W.E. 2003, *Enhancing the thermal design and optimization of SOFC technology*. Masters Thesis, Atlanta: Georgia Institute of Technology.
- SIMETRIC. *Summary: mass, weight, density, or specific gravity of water at various temperatures and thermal coefficient of expansion of water*. [Online] Available at: <http://www.simetric.co.uk/si_water.htm>. Accessed 24/04/2008.

- SCOTT, K.W., TAAMA, J. & CRUICKSHANK. 1997. *Performance and modeling of a direct methanol solid polymer electrolyte fuel cell*. Journal of Power Sources, 65:159–171.
- SCOTT, K., TAAMA W.M., ARGYROPOULOS, P. & SUNDMACHER, K. 1999. *The impact of mass transport and methanol crossover on the direct methanol fuel cell*. Journal of Power Sources, 83:204-216. [Online]. Available at: <<http://www.sciencedirect.com/>>. Accessed 15/03/07.
- SUNDMACHER, K., SCHULTZ, T., ZHOU, S., SCOTT, K., GINKEL, M. & GILLES E. D. 2001. *Dynamics of the direct methanol fuel cell (DMFC): experiments and model-based analysis*. Chemical Engineering Science, 56:333–341.
- SUNG MIN, C., CHAN-HWA, C., YOUNG-KWAN, L., JAE-DO, N., JUNG, H.J., CHONG, S.K., HYUNG, M.K. & HOO-GON, C. *3W DMFC System performances with a methanol sensing system*. Department of Chemical Engineering, Korea, Suwon: Sungkyunkwan University, p.440-746.
- SUZUKI, H. & OGAWA, K. 1991 *Development of an optical fuel composition sensor*. SAE Paper No. 910498, Society of Automotive Engineers, Warrendale, Pennsylvania.
- TEXAS INSTRUMENTS INCORPORATED. 2004. *TSPR2KXY-M methanol concentration sensor datasheet*. Texas instruments incorporated. Sensors and Controls. October 2004.
- VALDEZ, T.I. & NARAYANAN, S.R. 2000. *Recent studies on methanol crossover in liquid-feed direct methanol fuel cells*. NASA Technical Reports: Jet Propulsion Laboratory Energy Production and Conversion.
- WILKINSON, D.P., CHOW, D.E., ALLEN, E.P., JOHANNES, J.A., ROBERTS, J., ST-PIERRE, C.J., LONGLEY, J.K.K. & CHAN, J.K. 2000, *Method and apparatus for operating an electrochemical fuel cell with periodic fuel starvation at the anode* U. S. Patent 6,096,448.

Annexure A PIC source code for the controller

```
////////////////////////////////////
////          methcontrol.C          ////
////          ////
//// This program was written for the methanol fuel cell controller ////
//// to investigate the management possibility of methanol      ////
//// and the relation to output.          ////
////          ////
////          ////
////////////////////////////////////
//// (C) Copyright 2006 Marius Viljoen  ////
//// Vaal University of Technology      ////
////          ////
////////////////////////////////////
#include "C:\Program Files\PICC\Methanol\Methfinal.h"
#include <rs232>(baud=9600, xmit=PIN_C6, rcv=PIN_C7)

#define PIN_A3
#define PIN_A4
#define CIRC_ENABLE PIN_A5

#define RED_LED PIN_B0
#define GREEN_LED PIN_B1
#define BUZZER PIN_B2
#define METH_PUMP PIN_B3
#define SCALE_D0 PIN_B4 //cooling fan on radiator
#define SCALE_D1 PIN_B5 //cooling fan inside cabinet

#define SW PIN_C0
#define AIR_PUMP PIN_C1
#define CIRC_PUMP PIN_C2
#define TANK_LEV1 PIN_C3
#define TANK_LEV2 PIN_C4
#define TANK_LEV3 PIN_C5

#include <lcd4.c> // Driver for 4 Line LCD Display
#include <input.c>
#include <ds1820_18F452.c>

display_2Seconds(){
    delay_ms(2000);
    restart_wdt();
}

display_1Second(){
    delay_ms(1000);
    restart_wdt();
}

int16 Read_Sensors(int i) {
    int16 history[20];
    int x,count=20,y=0;
    float reading=0;
    //setup_port_a(A_ANALOG_RA3_RA2_REF);
```

```

    setup_port_a(ALL_ANALOG);
    setup_adc(ADC_CLOCK_DIV_32);
    set_adc_channel(i);
    delay_ms(100);
    reading=read_adc();
    for (x=1;x<=count;x++) {
        delay_us(25);
        history[y]=read_adc();
        reading += (float)history[y];
        y++;
    }
    reading /= count;
    setup_adc_ports(NO_ANALOGS); // To be able to use some of other pins for General I/O (3
    dae se sukkel)
    return (reading);
}

```

```

float mmix_test (float ma,float mb,float mc,float mtemp){
    float mmix_tst;
    mmix_tst=ma+(mb*mtemp)+(mc*mtemp*mtemp);
    return(mmix_tst);
}

```

```

void main()
{
    char k,strval,strdata[20];
    byte temp_set,value,pump_time,range;
    int i,meth_use,circ_speed=60,circ_time=10,circ_val,meth_total,meth_val=4;
    int disp_setting,temp_count=1,temp_result[20];
    int16 meth_pump_on,initial_flag=0;
    float Vdet,Vtmp,temp_air,Det_V,Temp_L,mmix,mmixold,temp_dif;
    short scale_set=0;

```

```

    setup_adc_ports(NO_ANALOGS);
    setup_adc(ADC_OFF);
    setup_psp(PSP_DISABLED);
    setup_spi(FALSE);
    setup_wdt(WDT_OFF);
    setup_timer_0(RTCC_INTERNAL);
    setup_timer_1(T1_DISABLED);
    setup_timer_2(T2_DISABLED,0,1);
    setup_timer_3(T3_DISABLED|T3_DIV_BY_1);
    setup_oscillator(False);

```

```

    lcd_init();

```

```

    output_high(BUZZER);
    output_high(GREEN_LED);
    lcd_putc("\fMethanol Mixer");
    lcd_putc("\nTest System");
    lcd_putc("\nVersion 4.080713");
    lcd_putc("\nM VILJOEN");
    display_2Seconds();
    output_low(BUZZER);
    output_low(SCALE_D1);
    output_high(SCALE_D0);

```

```

output_high(GREEN_LED);
lcd_putc("\fSystem Ready...\n");
lcd_putc("\nVAAL UNIVERSITY");
lcd_putc("\nOF TECHNOLOGY");

```

```

// Setup motor speed control for circulation pump
setup_ccp1(CCP_PWM);
setup_timer_2(T2_DIV_BY_4, 127, 1); //(1/4000000)*4*4*128 = 512 us or 1.9 khz
set_pwm1_duty(circ_speed);
output_high(CIRC_PUMP);
output_high(CIRC_ENABLE);

```

```

while(True) {
    if (initial_flag == 1){
        scale_set=0;
        output_low(SCALE_D1);
        output_high(SCALE_D0);
        Vdet=(float)Read_Sensors(0);
        if (Vdet>740){
            scale_set=1;
        }
        if (scale_set==1){
            output_high(SCALE_D1);
            output_low(SCALE_D0);
            Vdet=(float)Read_Sensors(0);
            Vdet=Vdet+360;
        }
        Det_V=(Vdet*4.6192506+9.0563393) ;
    }

    if (initial_flag == 2){
        Vtmp=(float)Read_Sensors(1);
        Temp_L=(Vtmp*0.16325)-49.5786;
        temp_count++;
        disp_setting=0;
        temp_result[temp_count]=(int)Vtmp;
        If (temp_count>20) temp_count=0;
        temp_dif=(float)temp_result[2]-(float)temp_result[18];
        if (temp_dif>3) disp_setting=1;
        if (temp_dif<-3) disp_setting=1;
    }

    if (initial_flag == 4){
        float a,b,c;

        meth_total=88;
        a=1979.3569;
        b=-5.2679035;
        c=0.003815472;
        mmix=mmix_test(a,b,c,Vtmp);
        if (Vdet>=mmix){ //9% Test
            a=2136.3909;
            b=-5.6845152;
            c=0.004115152;
            meth_total=10;
            mmixold=mmix;

```

```

}
mmix=mmix_test(a,b,c,Vtmp);
if (Vdet>=mmix){ //8% Test
    a=2318.6455;
    b=-6.1818485;
    c=0.004478788;
    meth_total=9;
    mmixold=mmix;
}
mmix=mmix_test(a,b,c,Vtmp);
if (Vdet>=mmix){ //7% Test
    a=2495.8091;
    b=-6.6637273;
    c=0.004830303;
    meth_total=8;
    mmixold=mmix;
}
mmix=mmix_test(a,b,c,Vtmp);
if (Vdet>=mmix){ //6% Test
    a=2672.9636;
    b=-7.1423636;
    c=0.005175758;
    meth_total=7;
    mmixold=mmix;
}
mmix=mmix_test(a,b,c,Vtmp);
if (Vdet>=mmix){ //5% Test
    a=2839.9636;
    b=-7.5784242;
    c=0.005478788;
    meth_total=6;
    mmixold=mmix;
}
mmix=mmix_test(a,b,c,Vtmp);
if (Vdet>=mmix){ //4% Test
    a=3010.9818;
    b=-8.0289697;
    c=0.005793939;
    meth_total=5;
    mmixold=mmix;
}
mmix=mmix_test(a,b,c,Vtmp);
if (Vdet>=mmix){ //3% Test
    a=3209.0182;
    b=-8.5955152;
    c=0.006230303;
    meth_total=4;
    mmixold=mmix;
}
mmix=mmix_test(a,b,c,Vtmp);
if (Vdet>=mmix){ //2% Test
    a=3494.6956;
    b=-9.4968668;
    c=0.006982749;
    meth_total=3;
    mmixold=mmix;
}

```

```

    }
    mmix=mmix_test(a,b,c,Vtmp);
    if (Vdet>=mmix){ //1% Test
        a=3546.5909;
        b=-9.4846364;
        c=0.006854546;
        meth_total=2;
        mmixold=mmix;
    }
    mmix=mmix_test(a,b,c,Vtmp);
    if (Vdet>=mmix){ //0% Test
        a=3742.5364;
        b=-10.041061;
        c=0.007278788;
        meth_total=1;
        mmixold=mmix;
    }
    mmix=mmix_test(a,b,c,Vtmp);
    if (Vdet>=mmix){ //0% Test
        meth_total=0;
        mmixold=mmix;
    }
}

if (initial_flag >= 6){
    temp_air=(float)onewire_ds1820_read(1);
    temp_air=temp_air/2+0.05;
    //if (temp_air>=30) output_high(FAN2); // Switch on air cooling Fan
    //else if (temp_stack<=28) output_low(FAN2);
}

if (initial_flag == 8){
    printf(lcd_putc, "\fDet_V=%4.0f      %u mV", Det_V, scale_set);
    printf(lcd_putc, "\nMix Temp=%2.1f  %2.1f", Temp_L, temp_air);
    printf(lcd_putc, "\nMethanol Vol: %u %%", meth_total);
    if (disp_setting==0) printf(lcd_putc, "\n-OK-");
    if (disp_setting==1) printf(lcd_putc, "\nTemp not Stable:%3.0f", temp_dif);
    if (disp_setting==2){
        output_high(METH_PUMP);
        printf(lcd_putc, "\nAdding Methanol");
        delay_ms(900);
        output_low(METH_PUMP);
        initial_flag = 0;
    }
    //printf(lcd_putc, "\nVdet=%4.0f  %4.0f", Vdet, mmixold); temp_setting
    printf("\n\rVtmp: %3.0f; Temp_L: %4.2f; Vdet: %4.0f; mmix: %4.0f; MethVol:
%u;", Vtmp, Temp_L, Vdet, mmixold, meth_total);

}

if (initial_flag >= 30){
    if (meth_total<meth_val && disp_setting<0){
        disp_setting=2;
        initial_flag = 6;
    }
}
else {

```



```

        initial_flag = 0;
    }

}
while(!input(SW)){
    meth_val ++;
    if (meth_val==11) meth_val=0;
    printf(lcd_putc,"\fSet Meth Vol: %u %%",meth_val);
    display_1Second();
    initial_flag = 0;
}
set_pwm1_duty(circ_speed);
initial_flag ++;
restart_wdt();

}
}

```

Annexure B Murata Sensor Data Sheet



Concept

KNF micro diaphragm liquid pumps are based on the principle of the oscillating displacement pump which is remarkably simple in design. The circular power from the motor is converted into vertical movement by an eccentric. This motion is then transferred to a diaphragm by means of a connecting rod which in conjunction with an inlet and outlet valve creates a pumping action.

NF 10/11 type liquid pumps can be mounted in any position and can deliver up to 0.1 l/min depending on the model and will operate against pressures of up to 10 mWg.

The KNF modular system contains a wide standard range of materials, motors, voltages and frequencies to enable the selection of an optimal solution for your application.



Features

Small and powerful

Micro design and maximum performance resulting from built-in technology are the outstanding characteristics of this product.

Self-priming and excellent for pressure

Sophisticated diaphragm technology and precise valve structures enable performances of up to 3 mWg suction and 10 mWg pressure.

Extreme chemical resistance

The use of chemically resistant materials such as PTFE, PVDF, FFPM or other material combinations for the parts which come in contact with the liquid allows almost all neutral or corrosive liquids to be pumped.

Dry running, durable and maintenance free

The carefully considered design of these pumps allows them to be run dry and ensures safe operation and a long life even under the most severe conditions.



Areas of use

The versatility of KNF pumps allows a wide field of applications to be covered. Over many years our pumps have proved themselves in the following areas:

Analysers

- Medical / pharmaceutical
- Environmental / water treatment
- Food / toxicology

Laboratory

- Filtration
- Chromatography

Cleaning industry

- Cuvette cleaning
- Sterilisers
- Industrial washing machines

Printing

- Ink jet printing
- Photographic / film development

Other applications for diaphragm liquid pumps include: fuel cells, hydrogen generators, CD coating, dental technology, textiles and many more.

Performance Data			
Type	Flow rate (l/min)	Suction head (mWg)	Pressure head (mWg)
NF 10/11	■ 0.1	3 ■	■ 10

The KNF Modular Concept of Selection



General note

This Data Sheet provides an overview of the options with our NF 10/11 pumps. Certain standard options will be explained in more detail where necessary.

Flow curves

The flow curves illustrate how the flow rate alters in relation to the pressures before and after the pump. In the case of a combination of both we would be very happy to advise what the expected flow rate would be.

The values given in the curves are dependant upon the liquid, choice of head materials and the type of hoses being used. Therefore a certain deviation is to be expected.

Note: The flow rate is measured with water at 20°C.

1 Materials of head components

KNF FLODOS offers a wide range of different materials for those parts which come in contact with the liquid thus allowing the possibility of pumping most liquids.

2 Motors

E Shaded pole motor (AC)

DC Direct current motor

DCB Brushless direct current motor

NF 11 Ironless direct current motor

This provides the following advantages compared to a conventional DC motor: higher durability, less power consumption and smaller size.

3 Voltages / Frequencies

Choose from the different electrical connection possibilities. Special variations are available.

Modules

Our versatile self-selection program allows you to personally determine the optimum characteristics that you require from your pump. Select your diaphragm pump from the following characteristics:

Pump type			
Basic model	Components		
	1	2	3
NF 10/11			

1	Materials of head components	
KP	Head	PP
	Valves	EPDM
	Diaphragm	EPDM
	Resonating diaphragm	EPDM
KV	Head	PP
	Valves	FPM
	Diaphragm	FPM
	Resonating diaphragm	FPM
KT	Head	PP
	Valves	FFPM
	Diaphragm	PTFE
	Resonating diaphragm	FFPM
TV	Head	PVDF
	Valves	FPM
	Diaphragm	FPM
	Resonating diaphragm	FPM
TT	Head	PVDF
	Valves	FFPM
	Diaphragm	PTFE
	Resonating diaphragm	FFPM

2	Motoren
E	Shaded pole motor (AC)
DC	Direct current motor
DCB	Brushless direct current motor

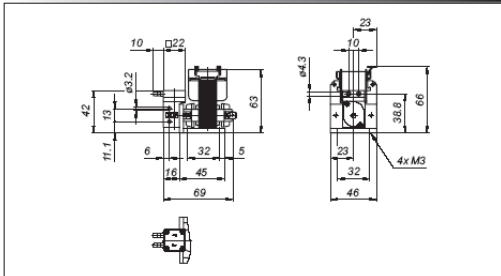
3	Voltages / Frequencies
230V / 50Hz 115V / 60Hz 100V / 50-60Hz	for AC motors
6 / 12 / 24V	for DC motors
12 / 24V	for DCB motors

Performance

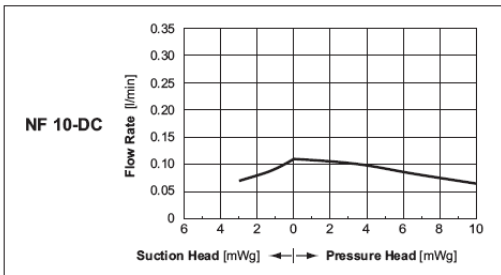
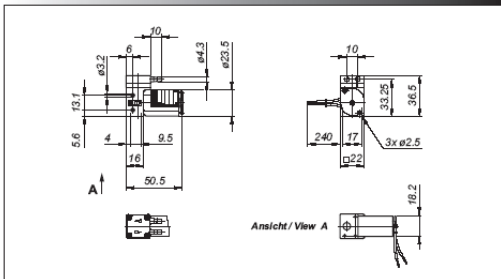
Basic model	Flow rate at atmos. pressure (l/min)	Max. suction head (mWg)	Max. pressure head (mWg)
NF 10-E	0.1	3	10
NF 10-DC	0.1	3	10

Motor selection	E	DC (NF 10)
Voltage (V)	230V / 50 Hz	6 / 12 / 24
Power rating (W)	9.1	3.8 / 3.7 / 3.4
I Last max. (A)	0.06	0.61/0.28/0.13
I max. (A)	0.08	0.64/0.31/0.14
EMC guideline	EN 55014	EN 55014
Motor protection factor	IP 00	IP 30
Weight	410 g	60 g

NF 10-E



NF 10-DC

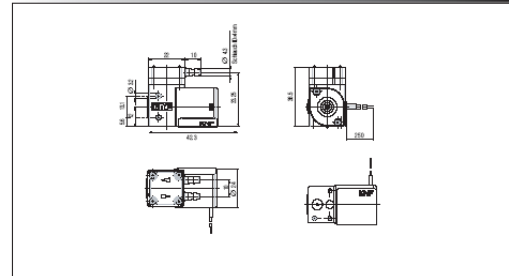


Performance

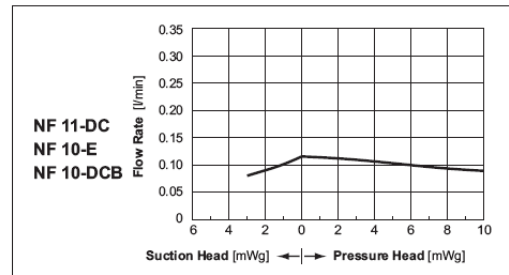
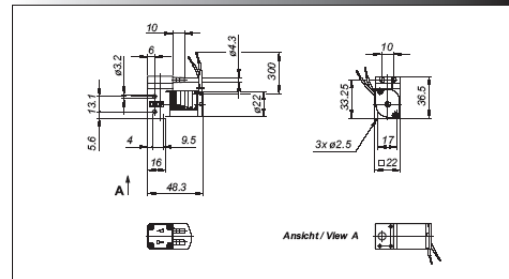
Basic model	Flow rate at atmos. pressure (l/min)	Max. suction head (mWg)	Max. pressure head (mWg)
NF 10-DCB	0.1	3	10
NF 11-DC	0.1	3	10

Motor selection	DCB (NF 10)	DC (NF 11)
Voltage (V)	12 / 24	6 / 12 / 24
Power rating (W)	2.0 / 2.4	2.2 / 2.5 / 2.3
I Last max. (A)	0.17 / 0.1	0.33/0.17/0.08
I max. (A)	0.17 / 0.1	0.37/0.21/0.09
EMC guideline	EN 55011 EN 61000-6-1	EN 55022 EN 55011
Motor protection factor	IP 30	IP 33
Weight	52 g	70 g

NF 10-DCB



NF 11-DC



Options



The NF 10/11 pump range comes with many other options. If you require any further information concerning the following features, our local sales representative would be very happy to be of assistance.



Special hose connections

UNF 1/4" - 28

Compression fitting for ID 4mm; OD 6mm hosing

Accessories

- Pulsation damper
- Pressure control valve / check valves
- Hoses
- Hose connections
- Shock mounts

Further options

- Suitable for pressures over 1.0 bar
- Other head materials
- Motors with special voltages and frequencies
- The incorporation of customers special requirements, for example special electrical connections (Molex, AMP, etc.)

KNF FLODOS AG, Wassermatte 2, 6210 Sursee, Switzerland
Telephone ++41 (0)41 925 00 25, Fax ++41 (0)41 925 00 35
www.knf-flodos.ch, info@knf-flodos.ch

INNOVATIVE
TECHNOLOGY
WORLDWIDE



Technical status: 12/2004
KNF FLODOS reserves the right to make technical changes.

Printed in Switzerland
ID No. 069 193